Ball J. et al. (2004) *Evaluating Remedial Alternatives for the Alamosa River and Wightman Fork, near the Summitville Mine, Colorado: Application of a Reactive-Transport Model to Low- and High-Flow Simulations.* Chapter 3 of *Environmental Sciences and Environmental Computing. Vol. II* (P. Zannetti, Editor). Published by The EnviroComp Institute (http://www.envirocomp.org)

Chapter 3

Evaluating Remedial Alternatives for the Alamosa River and Wightman Fork, near the Summitville Mine, Colorado: Application of a Reactive-Transport Model to Low- and High-Flow Simulations

James W. Ball, Robert L. Runkel, and D. Kirk Nordstrom

U.S Geological Survey, 3215 Marine Street, Boulder, CO 80303
jwball@usgs.gov, runkel@usgs.gov, dkn@usgs.gov

Abstract

Reactive-transport processes in Wightman Fork and the Alamosa River downstream from the Summitville Mine, south-central Colorado, were simulated at low and high flow using the OTEQ reactive-transport model. The simulations were calibrated using data from synoptic studies conducted during October 1998 and June 1999. Discharge over the 30-km reach from just below the mine site to the Alamosa River above Terrace Reservoir ranged from 0.077 to 1.3 m^3/s at low flow and from 1.17 to 17.0 m^3/s at high flow. Travel time was about 28 hours at low flow and about 8.5 hours at high flow; pH ranged from 4.6 to 5.7 at low flow and from 3.7 to 6.7 at high flow. Simulations revealed that pH, Fe, Al, and Cu were non-conservative. Simulations included Fe(II) oxidation, constrained using measured values of Fe(II) and Fe(total). Precipitation of hydrous Fe oxides and hydrous Al oxides and hydroxysulfates match observed conditions more closely in simulations that included Fe(II) oxidation and Fe(III) precipitation than in simulations without Fe(II) oxidation or Fe(III) precipitation. Simulation results indicate that sorption is controlling Cu concentrations in the Alamosa River. The calibrated models were used to evaluate nine remediation alternatives.

Key Words: reactive transport; hydrous metal oxides; mountain streams; iron; aluminum

© The EnviroComp Institute 2004

1 Introduction

Reactive-transport modeling can provide quantitative estimates of downstream attenuation of trace metals in acid mine waters under varying flow conditions. Such modeling can account for geochemical processes that may remove trace metals during transport and can be used to examine the effectiveness of potential remediation scenarios, providing a scientific basis for environmental and regulatory decisions.

The Summitville Mine is located along upper Wightman Fork in south-central Colorado (fig. 1). Gold was first discovered at Summitville in 1870 (King 1995). Until about 1985, gold was extracted from the deposit using conventional underground mining techniques, including sinking shafts, removing the ore, and transporting it to smelters for refining. More recently, highly disseminated gold was recovered by the cyanide heap-leach process. This process consists of placing relatively low-grade ore on a large pad and spraying a sodium cyanide solution over the top of the ore. The leachate solution percolates through the ore by gravity, then is recovered from the bottom of the pad and transported to a central area where the gold is removed from the cyanide solution. Much of the residual rock contains sulfide minerals that can oxidize rapidly to form acid mine water with high sulfuric acid concentrations that can be toxic to plants and animals living downstream. An aerial photograph of the mine workings, demonstrating the extent of removal of the mountainside, is shown in figure 2.

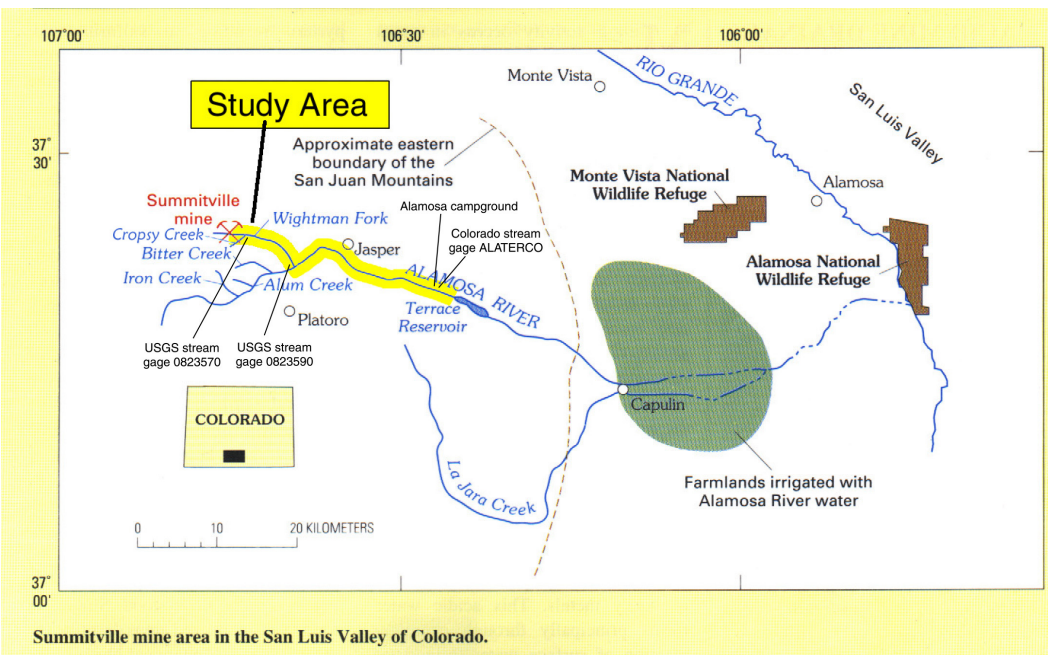

Figure 1. Schematic drawing of the Summitville Mine area (from King 1995)

In December 1992, following several catastrophic releases of acidic water from the site containing toxic concentrations of cyanide and heavy metals, the Colorado Department of Public Health and Environment (CDPHE) halted mining operations and requested assistance

from the U.S. Environmental Protection Agency (EPA), including authorization of Superfund Emergency Response. In 1993, the U.S. Geological Survey (USGS) began water-quality investigations at Summitville, Terrace Reservoir, and farther downstream (fig. 1; King 1995, Walton-Day et al. 1995, Balistrieri et al. 1996, Stogner et al. 1996). The USGS began routine water-quality monitoring and detailed water-quality characterization in the upper Alamosa River (Alamosa River and tributaries above Terrace Reservoir) in 1995, including two tracer-injection and synoptic studies in upper Wightman Fork above the Summitville mine (Ortiz and Bencala, 2000; Ortiz and Ferguson, 2000; Ortiz and Stogner, 2000; Ortiz, 2001; Rupert, 2001).

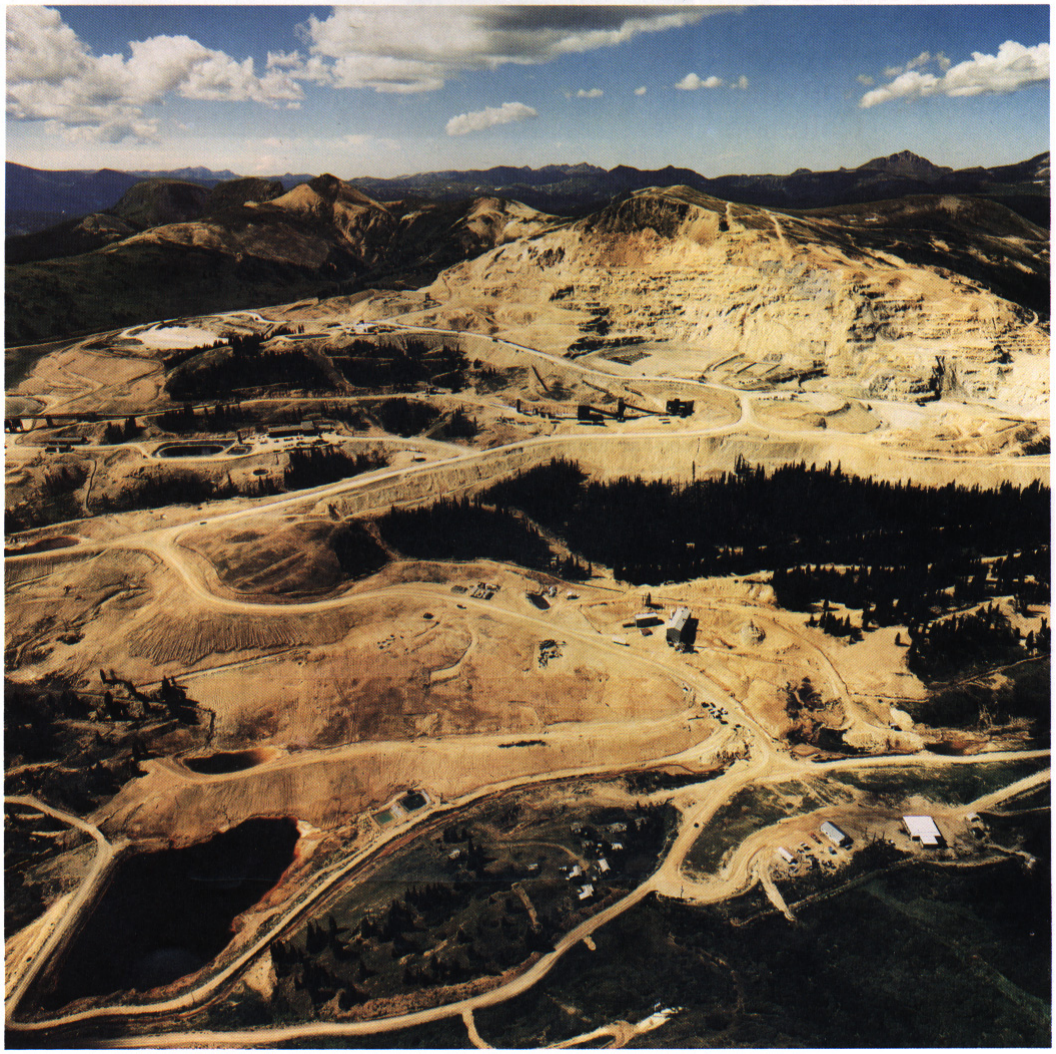

Figure 2. Aerial photograph of the Summitville Mine workings, August, 1994 (from King 1995). Holding pond is the large, dark feature at the lower left corner of the photograph.

In mid-1998, CDPHE assumed management of the site, and began working with the USGS to characterize the Alamosa River system from Wightman Fork below the Summitville Mine to the Alamosa River above Terrace Reservoir. The ultimate goal was to devise a long-term

remediation strategy that would allow restoration of the Alamosa River and Wightman Fork to near pre-mining conditions.

The USGS began a reactive-transport modeling investigation in 1998 that included preliminary OTEQ modeling of 1997 data (Ball et al., 1999). Low-flow and high-flow model calibrations are described by Nordstrom et al. (1999), Ball et al. (2000a) and Ball et al. (2000b), respectively. Use of the calibrated high-flow model to simulate sorption of Cu to the quantity of hydrous ferric oxide actively forming in the water column is described by Ball et al. (2001). In the Alamosa River Basin, two synoptic studies with tracer injection helped quantify solute sources and sinks, and allowed calibration of models and simulations of reactive transport under several remediation scenarios. The results of this investigation were used by EPA and CDPHE to design regulatory requirements and to achieve water-quality goals for the Alamosa River/Terrace Reservoir system. The purpose of this paper is to describe calibration of the reactive-transport model using data from synoptic studies conducted in October 1998 and June 1999, and application of the transport simulations to evaluation of remediation scenarios.

2 Methods

A chronicle of sampling activities for the two tracer-injection synoptic studies in the Summitville Mine area is presented in Table 1. At low flow in October 1998 (low-flow study) a tracer injection was done by introducing a slug of concentrated NaCl solution into Wightman Fork downstream from its confluence with Cropsy Creek and monitoring the increase in the Cl concentration at two points along Wightman Fork. Synoptic sampling of the Wightman Fork and Alamosa River main stems and tributaries was done on October 15, 27, and 28.

In June 1999 (high-flow study) a tracer injection at high flow was accomplished by pumping a concentrated NaCl solution into Wightman Fork for 30 hours at a constant rate. After tracer concentrations reached steady state, synoptic samples were collected from 28 tributaries and at 21 stream sites along the main stem of Wightman Fork and the Alamosa River. Chloride concentrations from the synoptic samples were used to determine stream discharge using the tracer-dilution method (Runkel and Kimball, 2002) as detailed in section 3.5.2.

At both low and high flow a slug tracer injection of rhodamine dye was used to monitor flow and mixing in the Alamosa River from its confluence with Wightman Fork to Terrace Reservoir. A pumped tracer injection was impractical for the Alamosa River because of its high discharge. Analytical results from low-flow and high-flow synoptic samples were used for calibration of the OTEQ model, a solute-transport framework that couples a one-dimensional transport model with a chemical equilibrium submodel (Runkel et al., 1996a; 1996b; 1999).

2.1 Sample Collection, Stabilization, and Analysis

2.1.1 Sampling Locations

The study area is bounded within the Alamosa River Basin. The emphasis of the study was on two stream segments, one each on the Alamosa River and Wightman Fork. The first is a 7.7-km segment of Wightman Fork from below the Summitville Mine downstream to the confluence with the Alamosa River (fig. 1). The second is a 22.5-km segment of the Alamosa River from downstream of Wightman Fork to upstream of Terrace Reservoir (fig. 1)

Sampling station IDs were developed from abbreviations of the stream name followed by a numerical value indicating its location in river miles upstream from the mouth of the stream (Ortiz and Ball, 2003a; 2003b). As an example, AR34.5 corresponds to a site on the Alamosa River 34.5 miles from its confluence with the Rio Grande. River mile designations for existing sites were found to be in error while determining river miles for new sampling sites for the October 1998 and June 1999 studies on the Alamosa River and Wightman Fork. Therefore, river mile designations were re-evaluated for all historical sites upstream from Terrace Reservoir. To avoid the confusion of a single site having multiple site IDs, a new identifier was defined. The new identifier was called the river mile ID (rmID). The nomenclature of the new identifier was similar to previous site IDs. The rmID was developed from abbreviations of the stream name followed by a lower case 'm' to indicate river miles, and a numerical value indicating its actual river mileage upstream from the mouth of the stream (Table 1). As an example, ARm35.4 corresponds to a site on the Alamosa River 35.4 miles from its confluence with the Rio Grande; historically, this site was identified by AR34.5. River-mileage estimates for the October 1998 sampling were re-evaluated prior to the June 1999 sampling event because of the availability of better methods to determine more precise river-mileage estimates. Therefore, several river-mile IDs changed slightly between the low-flow and high-flow sampling events. Several tributaries on the Alamosa River and Wightman Fork designated as unnamed on USGS 7.5-minute topographic maps were given names for the purpose of site identification. This evaluation was conducted using a geographic information system (GIS). Sites were identified on maps, digital representations of the maps were constructed, and distances between sampling points were determined.

Table 1. Sampling activities for the low-flow and high-flow tracer-injection synoptic studies

Date	Activity	Purpose
15-Oct-98	Synoptic sampling and stream gaging of south side Wightman Fork tributaries	Collect samples and gage stream flows before onset of impending snowstorms
27-Oct-98	Synoptic sampling and stream gaging of Alamosa River and tributaries	Collect onsite water-quality parameters and samples, gage stream flows
28-Oct-98	Rhodamine dye tracer injection in the Alamosa River	Obtain travel time estimates for the Alamosa River between Wightman Fork and Terrace Reservoir
28-Oct-98	Synoptic sampling and stream gaging of Wightman Fork main stem and north side tributaries	Collect onsite water-quality parameters and samples, gage stream flows
29-Oct-98	Slug sodium chloride tracer injection in Wightman Fork	Obtain travel time estimates for Wightman Fork between WFm4.8 and the Alamosa River
9-Jun-99	Rhodamine dye tracer injection in Wightman Fork, begun at 09:00	Obtain travel time estimates for Wightman Fork between WFm4.8 and the Alamosa River
9-Jun-99	Rhodamine dye tracer injection in the Alamosa River, begun at 10:03	Obtain travel time estimates for the Alamosa River between Wightman Fork and Terrace Reservoir
10-Jun-99	Continuous constant-rate sodium chloride tracer injection in Wightman Fork, begun at 10:45	Establish steady-state injection of Cl for tracer dilution flow calculations
10-Jun-99	Synoptic sampling and stream gaging of Loki, Steep, Elephant Mountain, Nickel, Fall, and California Gulches and Brewer Creek	Collect onsite water-quality parameters and samples, gage stream flows
11-Jun-99	Synoptic sampling and stream gaging of Wightman Fork and Alamosa River main stem sites and remaining tributaries	Collect onsite water-quality parameters and samples, gage stream flows
11-Jun-99	Sodium chloride tracer injection in Wightman Fork terminated at 15:00	Sampling completed

2.1.2 Measurement of Onsite Parameters

Instantaneous streamflow measurements were made at all tributary sites and at selected sites on the mainstem of the Alamosa River and Wightman Fork. Discharge measurements were made using approved USGS methods (Buchanan and Somers, 1969). These included equal width increment (EWI) methods and volumetric measurements. In general, USGS stream gaging equipment was used, although electromagnetic velocity meters also were utilized (Ortiz and Ball, 2003a; 2003b).

For the October 1998 tracer study, water temperature, specific conductance, and pH were measured at each synoptic site. Field meters were calibrated prior to collection of water-quality measurements. Specific conductance meters were calibrated using a minimum of three standards that bracketed the expected range of specific conductance for individual sites. Calibration of pH meters also was done with a minimum of two buffers that bracketed the expected pH range for an individual site. Meters usually were calibrated upon arrival at each site. However, if a selected site was near the previous site and field parameters were expected to be within similar ranges, meters were checked but recalibrated only if their calibrations had drifted.

For the June 1999 tracer study, instantaneous field parameters were measured at most sampling sites. The measured parameters, water temperature, specific conductance, and pH, were taken using field meters calibrated as specified in the previous paragraph. In addition, specific conductance and pH were measured at a central processing area using a single set of meters. These measurements are considered laboratory values because as many as several hours passed between sample collection and measurement of field parameters.

2.1.3 Sampling and Preservation

At high-discharge sites, samples were collected using EWI methods with DH-81 samplers and 8-L churns. For the low-discharge sites, multi-vertical or grab sampling at a centroid was used to collect representative samples in 1- or 3-L polyethylene bottles. In October 1998, samples were proccessed on-site, either from the back of an all-terrain vehicle in the Wightman Fork canyon or from dedicated sampling vehicles along the Alamosa River (Ortiz and Ball, 2003a).

In June 1999, because of high discharges and rapid travel times, most Wightman Fork and Alamosa River samples were multi-vertical or grab samples collected from the bank depending on accessibility and time and safety considerations. Samples from tributaries were collected using grab sampling from the centroid. Samples were transported to the central processing area for filtration and determination of specific conductance and pH.

Synoptic sample analyses included dissolved and total recoverable metals, anions, and alkalinity. At selected synoptic sites, Fe(II) and Fe(total) also were determined. Samples for determination of concentrations of dissolved metals, Fe redox species, and anions and alkalinity were filtered through a 0.45 μm-pore-size capsule filter using a peristaltic pump.

Mobile Fe, Al, Cu, and Zn concentrations represented dissolved plus suspended, or total recoverable, values determined by analyzing an unfiltered, acidified sample split.

Samples for dissolved and total recoverable metals were acidified to pH less than 2 with concentrated HNO_3. Samples for Fe(II) and Fe(total) determinations were acidified to pH less than 2 with 6 M HCl. No preservative was added to samples for dissolved anions and alkalinity titrations. All samples were maintained at 4 °C until analysis.

2.1.4 Analytical Methods and Quality Control

A list of analytes, analytical methods, and operational detection limits is presented in Table 2. Dissolved Fe(II) and Fe(total) were determined using a modification of the FerroZine method of Stookey (1970). Dissolved Fe(III) was determined for selected samples using the method of To et al. (1998). To ensure data validity, laboratory quality control (QC) samples were analyzed by the USGS analytical laboratory in Boulder, Colorado. These samples included method blanks, sample duplicates, and standard reference water samples. Laboratory QC samples were analyzed at a rate of 1 per 20 samples or one per analytical batch, whichever was the greater frequency, for all methods (Ortiz and Ball, 2003a; 2003b).

Table 2. Analytes and detection limits for tracer injection studies

Constituent	Method	Detection Limit (mg/L)	Upper Determination Limit (mg/L)[1]
Ca	ICP/OES[2]	0.1	20
Mg	ICP/OES	0.1	20
Na	ICP/OES	0.3	100
K	ICP/OES	0.6	20
SO_4	Ion Chromatography[3]	0.4	30
Alkalinity (as HCO_3)	H_2SO_4 Titration	1.0	200
F	Ion Chromatography	0.05	3
Cl	Ion Chromatography	0.05	15
Br	Ion Chromatography	0.1	5
NO_3	Ion Chromatography	0.2	15
SiO_2	ICP/OES	0.32	21
Al	ICP/OES	0.09	4
Fe(total) ICP	ICP/OES	0.02	2
Fe(total)	FerroZine Colorimetric	0.002	1.5
Fe(II)	FerroZine Colorimetric	0.002	1.5
Fe(III) Direct	Acetohydroxamic Acid Colorimetric	0.02	1.5
B	ICP/OES	0.04	5
Sr	ICP/OES	0.001	0.5
Ba	ICP/OES	0.007	0.5
Mn	ICP/OES	0.001	2
Zn	ICP/OES	0.004	1
Pb	ICP/OES	0.05	1
Be	ICP/OES	0.001	0.5
V	ICP/OES	0.006	1
Cr	ICP/OES	0.05	1
Co	ICP/OES	0.007	0.5
Ni	ICP/OES	0.01	0.5
Cu	ICP/OES	0.08	1
Cd	ICP/OES	0.004	0.5
As(total)	ICP/OES	0.3	20

[1] Limit above which dilution or use of reduced volumes is necessary

[2] ICP/OES, Inductively Coupled Plasma/Optical Emission Spectrometry; both dissolved and total recoverable concentrations of ICP analytes were determined

[3] Ion chromatography limits are for a 50-mL sample loop

3 Modeling Approach

One aspect of stream characterization is to describe the watershed in as much detail as possible, to understand both the stream hydraulics and the reactive chemistry. Reactive solute-transport modeling for this analysis uses the OTEQ model. The resultant model accounts for a variety of physical and chemical processes including advection, dispersion, transient storage, transport and deposition of water-borne solid phases, acid-base reactions, complexation, precipitation/dissolution, and sorption. Consideration of these processes provides a general modeling framework for the simulation of trace-metal fate and transport.

Applications of OTEQ to date have focused on the analysis of geochemistry and transport during pH-modification experiments (Kimball et al., 1994; Runkel et al., 1996b; Broshears et al., 1996; Runkel et al., 1999). These experiments represent dynamic conditions that mimic events such as episodic acidification, unplanned mine discharges (blowouts), and accidental spills (e.g., Achterberg et al., 1999). Analyses of these experiments have provided quantitative descriptions of trace-metal behavior as a pH pulse propagates its way through the hydrologic system (Broshears et al., 1996). Another application of interest is quantification of the processes that determine the steady-state profile of trace metals and pH (Runkel and Kimball, 2002). This application is especially important when considering the potential effects of remediation on stream-water quality.

In this paper, model application to steady-state data provides a means to describe the processes that control metal concentrations as well as the sources of metals and acidity. Given this quantitative description of existing conditions, additional simulations may be conducted to estimate stream-water quality that might be achieved under different remediation plans. Steady-state application of OTEQ to the Summitville Mine area low- and high-flow synoptic studies is described in this section.

3.1 Conceptual Model and Governing Transport Equations

The hydrologic transport submodel in OTEQ is based on the OTIS solute-transport model, a one-dimensional advection-dispersion equation with additional terms to account for lateral inflow and transient storage (Bencala and Walters, 1983; Runkel, 1998). Transient storage has been noted in many streams in which solutes are temporarily detained in small eddies and stagnant zones of water that are stationary relative to the faster moving water near the center of the channel. In addition, parts of the flow move solutes through the coarse gravel of the streambed and the porous areas within the stream bank. Lateral inflow represents additional water entering the main channel as overland flow, interflow, and ground-water discharge. Conservation of mass results in a set of partial differential equations (PDEs) describing the physical transport of multiple solutes.

The chemical equilibrium submodel in OTEQ is based on MINTEQA2 (Allison et al., 1991), an extension of the MINEQL model developed by Westall et al. (1976). Given analytical concentrations of the chemical components, MINTEQA2 computes the distribution of chemical species that exist within a batch reactor at equilibrium. These equilibrium computations include the precipitation and dissolution of solid phases as well as sorption

processes. The mass-balance and mass-action equations, describing the different solution-mineral equilibria, form a set of non-linear algebraic equations (AEs).

Coupling transport with chemical equilibrium results in a simultaneous set of AEs and PDEs. The sequential iteration approach (Yeh and Tripathi, 1989) solves the coupled set of equations by dividing each time step into a "reaction" step and a "transport" step. During the reaction step, the equilibrium submodel is applied to each segment in the study reach. Each segment represents a batch reactor wherein chemical equilibrium is assumed. The equilibrium submodel thus determines the solute mass in dissolved, precipitated, and sorbed forms. On the basis of this information, a transport step is applied in which the solute-transport model determines the physical transport of the mobile phases of each solute. Because the transport and reaction steps neglect the coupling of the transport and chemistry, the procedure iterates until a specified level of convergence is achieved.

The governing equations and solution algorithms used within the reactive solute-transport model are based on the following assumptions:

- Complexation, precipitation/dissolution, and sorption reactions are assumed to be in a state of both partial and local equilibrium (DiToro, 1976; Rubin, 1983).

- Solute mass is uniformly distributed over the stream's cross-sectional area such that one-dimensional transport is applicable. The physical processes that affect solute mass in each stream segment include advection, dispersion, lateral inflow, transient storage, and settling. All dissolved, precipitated, and sorbed species resident in the water column travel at the same advective velocity.

- Solute mass for each chemical component is distributed among five distinct phases. The first three phases represent dissolved, precipitated, and sorbed mass that is present in the water column. These three phases are mobile, in that they are subject to transport. The final two phases represent precipitated and sorbed mass that resides on the streambed or is attached to stationary debris in the stream channel; these phases are immobile and are not transported.

- Dissolved mass in the water column may form precipitates if the solution becomes oversaturated with respect to the defined solid phases. Any precipitated mass initially resides in the water column and is subject to solid-phase transport until it settles to the streambed or redissolution occurs. Precipitated mass may accumulate on the bed, however, as transported precipitates are subject to the force of gravity and settle at a rate defined by a settling velocity.

- Dissolved species may sorb to solid phases in the water column or to sorption sites on the streambed. Conversely, sorbed species may desorb from sites in the water column or on the streambed. Runkel et al. (1999) discuss additional assumptions relative to sorption.

The fundamental equations that govern reactive solute transport are derived based on the above assumptions. Governing equations are formulated in terms of the chemical components defined within the equilibrium submodel. The total component concentration, T, in M L^{-1}, is the sum of the five individual component phase concentrations, with each phase consisting of one or more chemical species:

$$T = C + P_w + P_b + S_w + S_b \tag{1}$$

where C is dissolved;
P_w is mobile precipitate;
P_b is immobile precipitate;
S_w is mobile sorbed; and
S_b is the immobile sorbed phase.

A summary of the processes considered for each phase is presented in figure 3, where the system is represented as two compartments. The water column compartment contains the three mobile phases, C, P_w, and S_w; the immobile substrate (the streambed or debris) constitutes the second compartment, containing the two immobile phases, P_b and S_b. The three mobile phases are subject to physical transport (advection, dispersion, transient storage, and lateral inflow), as represented by the transport operator, $L(T)$. The dissolved phase, C, takes part in precipitation/ dissolution and sorption/desorption reactions that occur within the water column (interactions with P_w and S_w). The dissolved phase also is affected by dissolution of precipitate from the immobile substrate and by sorption/desorption from immobile sorbents (interactions with P_b and S_b). Finally, C may increase or decrease because of external sources and sinks (gas exchange for example), as denoted by s_{ext}. The precipitated and sorbed phases in the water column settle in accordance with settling velocity v [$L\ T\text{-}1$].

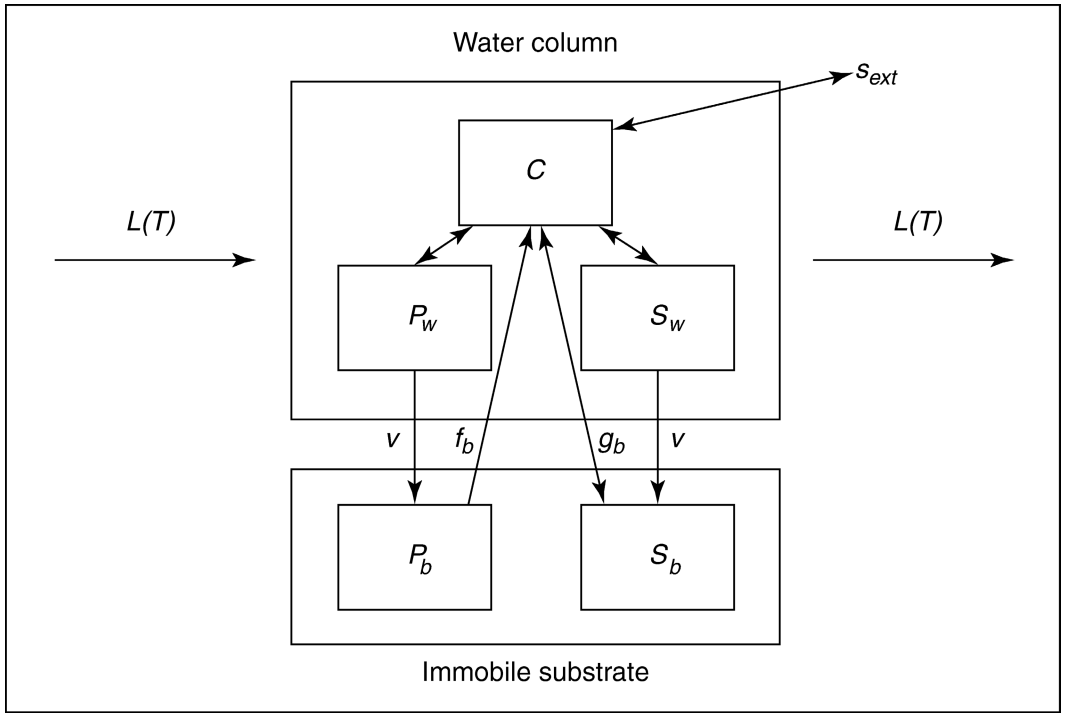

Figure 3. Conceptual model of a surface-water system. See text (section 3.1) for definition of terms.

The mass-balance equation for the total component concentration *T* is obtained by summing the mass-balance equations for the five individual component phases. This yields:

$$\frac{\partial T}{\partial t} = L(T) - L(S_b + P_b) + s_{ext} \tag{2}$$

where *L(T)* is the transport operator, defined in terms of the transient storage model (Bencala and Walters, 1983; Runkel, 1998) and s_{ext} *is a* source/sink term representing external gains and losses [moles/liter T^{-1}]. The immobile precipitated and sorbed concentrations in equation 2 are governed by:

$$\frac{\partial P_b}{\partial t} = \frac{v}{d}(P - P_b) - f_b \tag{3}$$

$$\frac{\partial S_b}{\partial t} = \frac{v}{d}(S - S_b) - g_b, \tag{4}$$

where

f_b is the source/sink term for dissolution from the immobile substrate ($M\ L^{-3}\ T^{-1}$),
g_b is the source/sink term for sorption-desorption from the immobile substrate ($M\ L^{-3}\ T^{-1}$),
v is the settling velocity ($L\ T^{-1}$),
d is the settling depth (L),
P is the total precipitate concentration (equal to P_w plus P_b), and
S is the total sorbed concentration (equal to S_w plus S_b).

The set of governing equations thus consists of three differential equations for each component (for T, P_b, and S_b) and the set of AEs representing chemical equilibria. This set of equations is solved by using a Crank-Nicolson approximation of the differential equations and the sequential iteration approach (Runkel et al., 1996a).

Model inputs include mixing parameters (dispersion and transient storage), streamflow estimates, lateral inflow concentrations, upstream boundary conditions, and geochemical parameters. Steady-state analyses under the assumption of chemical equilibrium are generally insensitive to mixing parameters, such that these parameters are not discussed here. The remaining inputs are discussed in sections 3.2 to 3.7. Most model inputs are allowed to vary spatially on a reach-by-reach basis.

3.2 Reaches

Each of the two stream segments (Wightman Fork and the Alamosa River) were divided into several model reaches for the transport simulations. A model reach is defined as a length of the stream with homogeneous physical properties in which model parameters are spatially constant. Each model reach is divided into several computational units (control volumes) to which the governing equations apply.

For both low-flow and high-flow transport simulations, the first model reach began at USGS sampling station WFm4.8 on Wightman Fork, just downstream from its confluence with Cropsy Creek, near USGS stream gage number 08235270. The Wightman Fork portion of the reach ended at USGS sampling station WF0.0 at the confluence of Wightman Fork and the Alamosa River (USGS stream gage number 08235290). The final model reach ended 200 m downstream from the Alamosa Campground, above Terrace Reservoir, near State of Colorado stream gage ALATERCO. Locations of these features are shown on figure 1.

Tributaries along the Alamosa River included the upper Alamosa River, Fall Gulch, Cornwall Creek, Dry Gulch, Donkey Gulch, Jasper Creek, Burnt Creek, Brewer Creek, Spring Creek, Fern Creek, Castleman Gulch, California Gulch, Silver Creek, Rough Canyon, Beaver Creek, Lieutenant Creek, Ranger Creek, French Creek, and Gypsy Gulch.

For the low-flow transport simulation, the two stream segments were divided into 56 model reaches (22 on Wightman Fork and 34 on the Alamosa River). At low flow, tributaries along Wightman Fork included Loki Gulch, Sawmill Creek, Steep Gulch, Big Hollow, Elephant Mountain Gulch, Palmer Gulch, Austin Gulch, Whitney Gulch, Smallpox Gulch, and Moss

Gulch (inflow to model reaches 2, 4, 6, 8, 11, 13, 15, 17, 19, and 21, respectively). Schematic diagrams of the low-flow model reaches for Wightman Fork and the Alamosa River are shown in figures 4 and 5, respectively.

For the high-flow transport simulations, the stream was divided into 42 reaches (26 on Wightman Fork and 16 on the Alamosa River). At high flow, tributaries along Wightman Fork included Helokrene Gulch, Estival Gulch, Loki Gulch, Sawmill Gulch, Steep Gulch, Big Hollow, Talus Spring, Greyback Mine, Elephant Mountain Gulch, Palmer Gulch, Austin Gulch, Whitney Gulch, Nickel Gulch, and Smallpox Gulch (inflow to model reaches 2, 4, 6, 8, 10, 12, 14, 18, 21, and 24, respectively). Schematic diagrams of the high-flow model reaches for Wightman Fork and the Alamosa River are shown in figures 6 and 7, respectively. Double lines represent tributary inflow locations, and single lines represent key sampling locations.

Several tributaries on the Alamosa River and Wightman Fork designated as unnamed on USGS 7.5-minute topographic maps were given temporary names for the purpose of site identification. Sampling station IDs were developed from abbreviations of the stream name followed by a numerical designation indicating its location, in river miles, upstream from the mouth of the particular stream. As an example, WFm4.8 corresponds to a site on Wightman Fork 4.8 miles from its confluence with the Alamosa River. The lower case "m" signifies that the river mile ID (rmID) is a river-mileage estimate and should not be confused with historical site nomenclature in the basin (e.g. WF5.5, AR34.5). River mileage estimates used for the low-flow sampling were re-evaluated prior to the high-flow sampling event because of the availability of better methods to determine more precise river-mileage estimates. Therefore, several river-mile IDs changed slightly (figs. 4-7). Sites were identified on 1:24,000 USGS topographic maps and distances between sampling points were determined using geographic information system (GIS) software (Ortiz and Ball, 2003a; 2003b).

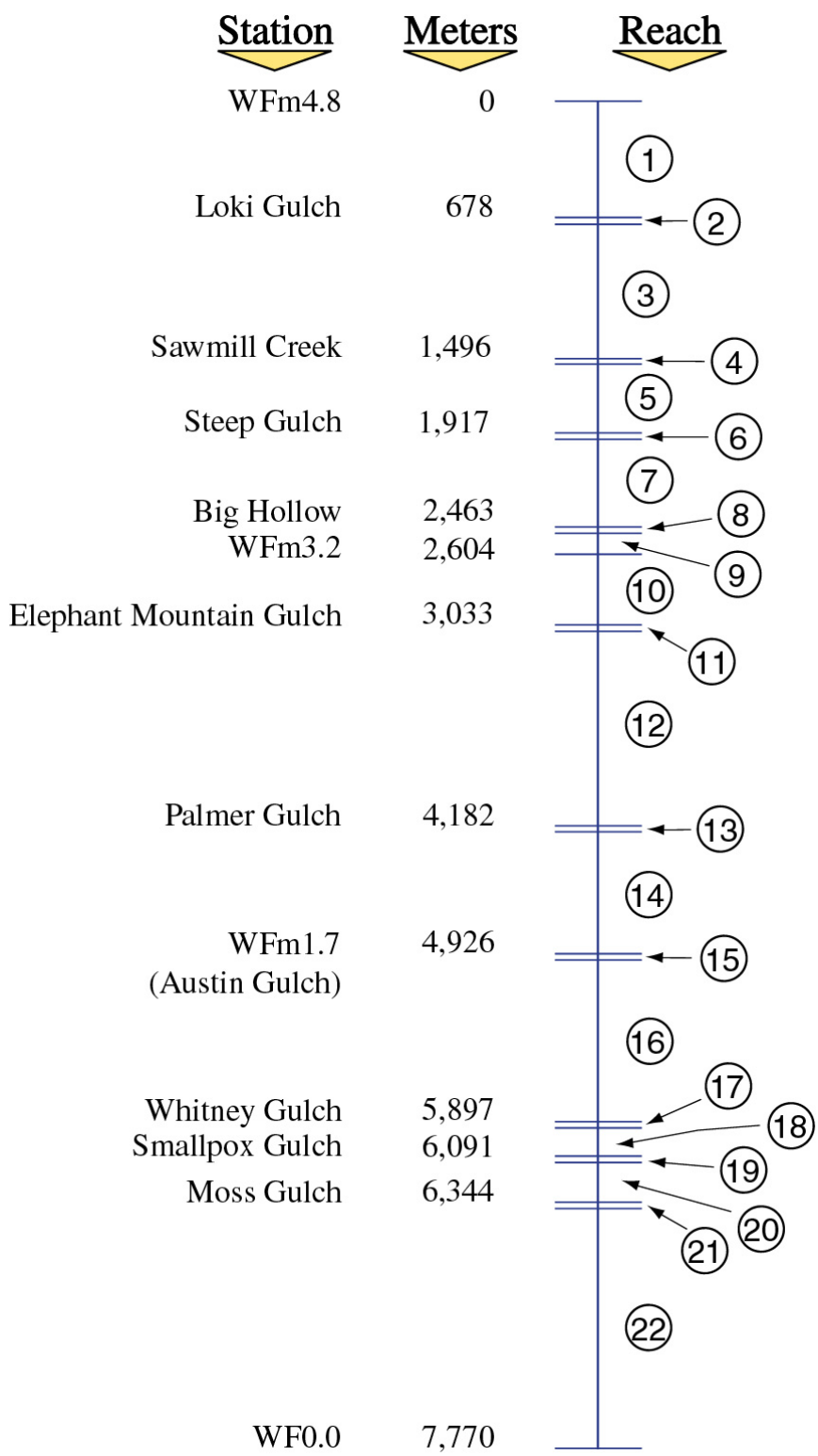

Figure 4. Schematic diagram of Wightman Fork model reaches for the low-flow transport simulations; circled numbers are model reach numbers

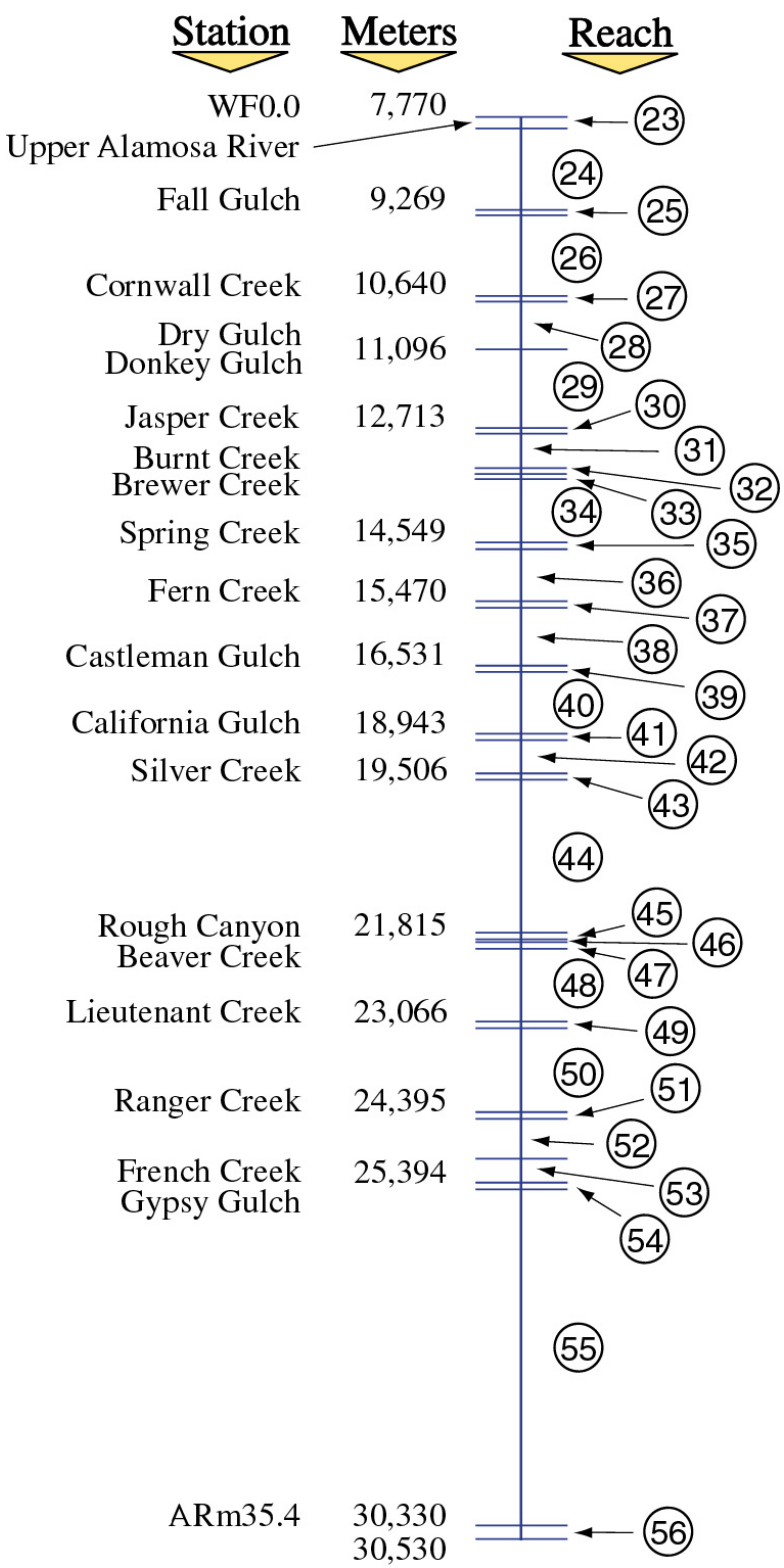

Figure 5. Schematic diagram of Alamosa River model reaches for the low-flow transport simulations; circled numbers are model reach numbers

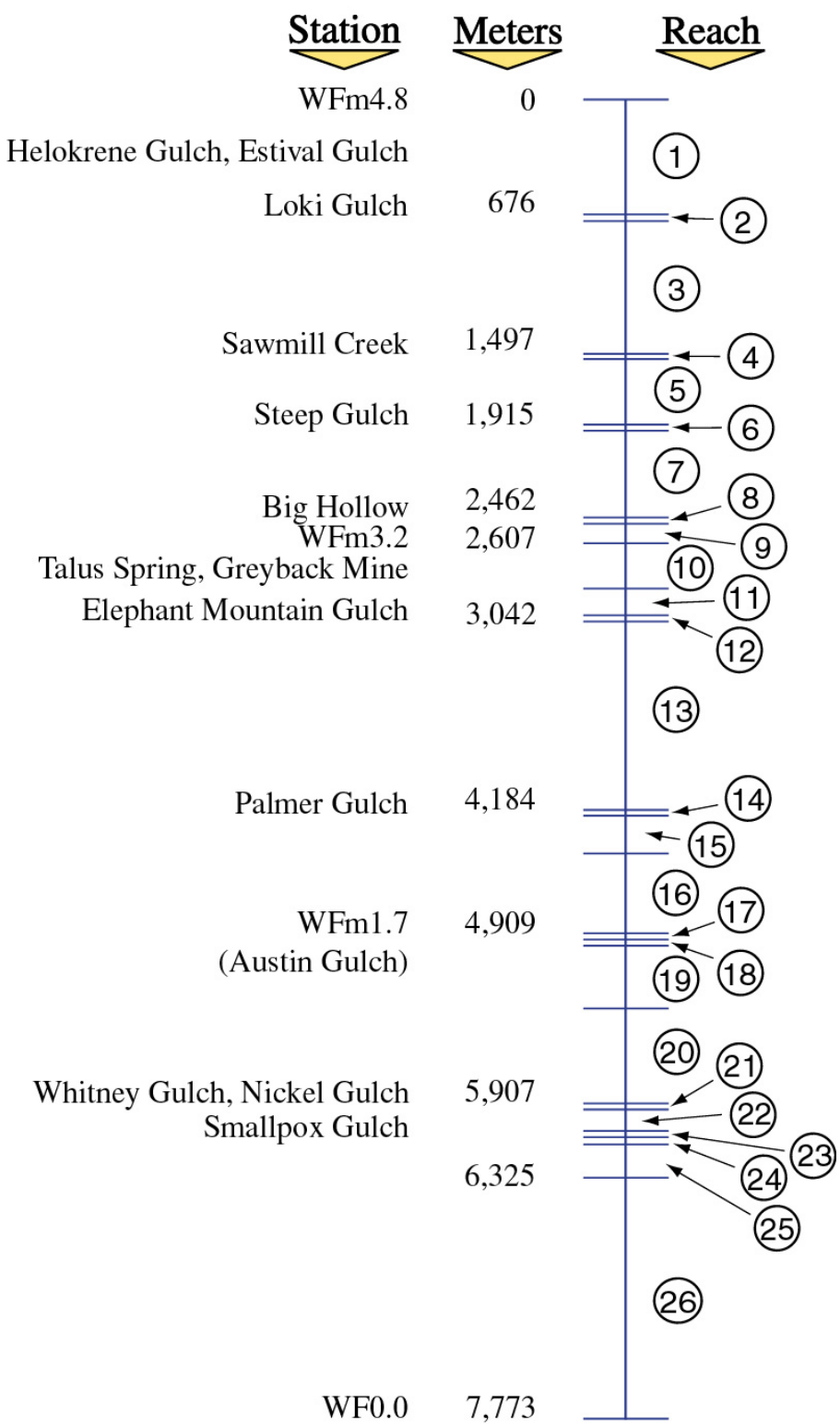

Figure 6. Schematic diagram of Wightman Fork model reaches for the high-flow transport simulations; circled numbers are model reach numbers

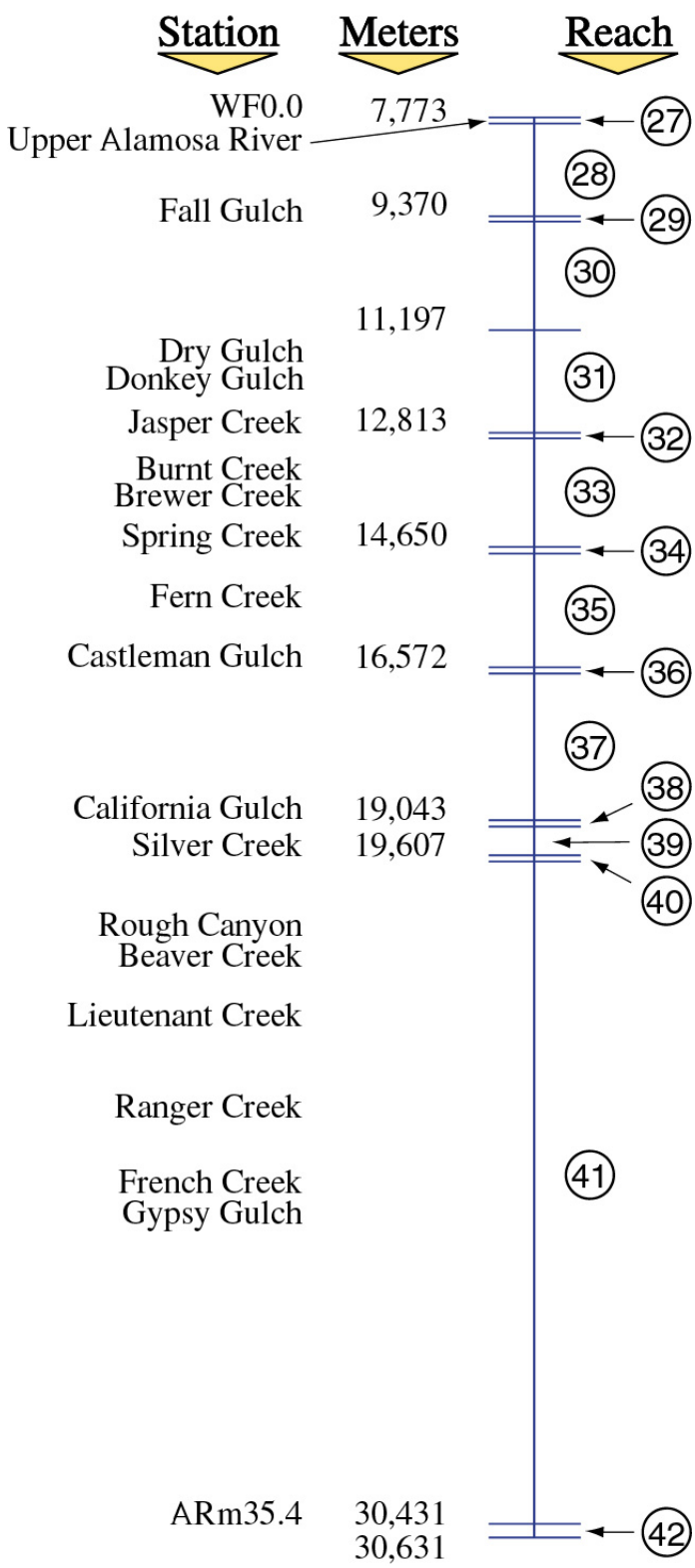

Figure 7. Schematic diagram of Alamosa River model reaches for the high-flow transport simulations; circled numbers are model reach numbers

3.3 Modeled Solutes and Sorbents

Initial OTEQ simulations were done using a 19-component set consisting of dissolved B, Ba, Ca, total inorganic carbon (TIC) as CO_3^{2-}, F, Fe(II), total excess H [H_T^+], K, Mg, Mn, Na, Ni, SiO_2, SO_4, Sr, and Zn; and total recoverable Al, Cu, and Fe(III). Of those, a subset of 12 components [dissolved Ca, total inorganic carbon (TIC) as CO_3^{2-}, F, Fe(II), total excess H [H_T^+], Mg, Mn, SO_4, and Zn; and total recoverable Al, Cu, and Fe(III)] was used. Total recoverable Fe(III) was calculated by differencing the total recoverable Fe and dissolved Fe(II) results. This approach is consistent with previous OTEQ simulations in other mine drainage streams (Broshears et al. 1996, Runkel et al. 1996b). Essentially identical simulation results (data not shown) based on the 19-component set demonstrated the correctness of the assumption that nonreactive components may be safely excluded from the simulations.

Transfer of mass between Fe(II) and Fe(III) resulting from redox processes was modeled by specifying, for each model reach, the fraction of total dissolved iron [Fe(II) + Fe(III)] that is Fe(II). The mass of sorbent within each stream segment was based on the amount of Fe(III) precipitated within the water column [suspended Fe(III)] in that segment, as determined by the chemical equilibrium submodel. In the simulations, all the Fe(III) precipitated within the water column remained in the water column, that is, none was settled to the stream bed. Precipitated Fe(III) on the streambed was assumed to be saturated with respect to sorbed species and therefore was not a sink in the steady-state analysis presented in this paper. Future substantial changes in Wightman Fork/Alamosa River water chemistry could require reconsidering this assumption.

3.4 Lateral Inflow Concentrations

Most reaches included one or more observed inflows that were used to set component inflow concentrations. When more than one inflow was available for a given reach, the largest observed inflow was generally used. TIC and H_T^+ were calculated for all surface inflow reaches by running MINTEQA2 simulations with pH fixed at observed values and with dissolved carbonate species either calculated from alkalinity titrations where available, or assumed to be at equilibrium with atmospheric CO_2. In surface inflow reaches, observed concentrations of dissolved Ca, F, Fe(II), Mg, Mn, and SO_4, and total recoverable Al, Cu, Fe(III), and Zn concentrations were used to set component inflow concentrations.

Of the 56 stream reaches considered for the low-flow simulation, 20 were “base flow” reaches for which no flow or chemistry information for the lateral inflow component existed. For these 20 reaches, inflow concentrations were estimated by averaging the compositions of the two nearest surface inflow sources. When necessary for the high-flow simulations, input values were estimated by setting them equal to the next downstream inflow source.

3.5 Streamflow Parameters

3.5.1 Low-Flow Streamflow

Streamflow estimates were based on instantaneous discharges measured at several points along Wightman Fork and the Alamosa River during the tracer-injection synoptic study. Discharges for Wightman Fork were measured on October 28, and discharges for its tributaries were measured on October 15 and 28, whereas the synoptic samples were collected on October 29. Snow storms prior to and through October 28, followed by a warming cycle, prohibited access to several isolated sites and resulted in considerable discharge variations in all the streams of the watershed. Consequently, discharges and chemical concentrations were not known with sufficient consistency for application to reactive-transport modeling. Thus, an approach was needed for obtaining improved discharge estimates that were both consistent and reasonable. One Wightman Fork tributary, Elephant Mountain Gulch, was sampled on both October 15 and 28. It was assumed that variations in streamflow between October 15 and 28 for the two Wightman Fork tributaries immediately upstream from Elephant Mountain Gulch were similar to those for Elephant Mountain Gulch. Accordingly, the value for the measured discharge of Steep Gulch was doubled prior to beginning calculations.

The confluence mass-balance approach was used to calculate discharges for Wightman Fork and selected tributaries. Wightman Fork was divided into three sections, the first from WFm4.8 to WFm3.2, the second from WFm3.2 to WFm1.7, and the third from WFm1.7 to WF0.0 (Table 3). For all three sections, SO_4, Ca, and Mg concentrations were assumed to be conservative and their measured concentrations were assumed accurate to within 5 percent. For the upper section only, it was assumed that the measured discharge of 77.3 L/sec at WFm4.8 was accurate, and that there were no lateral inflow sources other than the surface tributaries. Calculated discharge at the downstream end of each section was varied, and calculated discharges of the tributaries were constrained to vary proportionally to each other. The sums of the concentrations of SO_4, Ca, or Mg for the surface lateral inflows were calculated for each section using the following equation:

$$C_L = C_1 \times Q_1 / \Sigma Q_L + C_2 \times Q_2 / \Sigma Q_L + C_3 \times Q_3 / \Sigma Q_L + C_4 \times Q_4 / \Sigma Q_L , \qquad (5)$$

where

C_L	is the sum of all lateral surface inflow concentrations,
C_1 *to* C_4	are the SO_4, Ca, or Mg concentrations in tributaries 1 to 4,
Q_1 *to* Q_4	are the measured discharges for tributaries 1 to 4, and
ΣQ_L	is the sum of measured discharges for all tributaries in the section.

Any concentration and discharge units may be used, provided they are consistent throughout. Once C_L was calculated, the conservative mixing equation:

$$C_U \times Q_U + C_L \times Q_L = C_D \times Q_D , \qquad (6)$$

where

C_U, C_D are the respective main stem SO_4, Ca, or Mg concentrations at the upstream and downstream ends of the section,
Q_U, Q_D are the respective main stem discharges for the upstream and downstream ends of the section,
C_L is the summed lateral surface inflow SO_4, Ca, or Mg concentration calculated using eq (5), and
Q_L is the summed lateral surface discharge,

was solved for Q_D, the main stem discharge at the downstream end of the section. Finally, solving the conservation of mass of water equation for Q_L:

$$Q_L = Q_D - Q_U, \qquad (7)$$

where
Q_U, Q_D, Q_L have the same meanings as in equation (6),

yielded a new value for Q_L, the sum of the lateral inflows. The process was repeated for the three components, and the resulting Q_L values were averaged. This average summed Q_L was distributed among the tributaries proportionally, according to their initial measured discharges, and resulted in a new set of inflow discharge values. Accuracy of the initial calculation was confirmed by a second iteration that resulted in no discernible change in the recalculated discharges. Substituting the new main stem discharge at the downstream end of the section, the process was repeated for sections two and three. Model reaches, streamflows, and Fe(II) percentages used as low-flow model input are presented in Table 4.

Table 3. Initial and revised discharge values at low flow for the Wightman Fork model reach

Location ID	Discharge Measured on 10/28 [L s^{-1}]	Revised Discharge [L s^{-1}]	Change from Initial [Percent]	Base Flow [L s^{-1}]
WFm4.8	77.3	77.3	0	0
Loki Gulch	[1]2.3	1.9	-15	0
Sawmill Creek	[1]18.4	15.7	-15	0
Steep Gulch	[2]1.1	1.0	-15	0
Big Hollow	14.7	12.6	-15	0
WFm3.2	116	108	-6	2.0
Elephant Mtn Gulch	5.1	5.9	+17	5.4
Palmer Gulch	6.5	7.6	+17	3.5
WFm1.7	173	133	-26	0
Austin Gulch	7.9	9.2	+15	8.5
Whitney Gulch	5.1	5.9	+15	1.5
Smallpox Gulch	2.5	2.9	+15	2.0
Moss Gulch	[1]0.11	0.13	+15	12.6
WF0.0	189	176	-11	0

[1]Measured on 10/15/98.
[2]Estimate based on the 1/2 ratio (2.55 and 5.10 L s^{-1}) for the respective Elephant Mountain Gulch discharges measured on 10/15/98 and 10/28/98.

Table 4. Low-flow model reaches including streamflow, inflows, and Fe(II) percentages

Reach	Cumulative Distance [m]	Stream flow [L s^{-1}] Top of reach	Stream flow [L s^{-1}] Within reach increase	Observed inflows	Fe(II) percentage
1	678	77.3	0.0	none	90
2	708	77.3	1.9	Loki Gulch	90
3	1496	79.2	0.0	none	90
4	1526	79.2	15.7	Sawmill Creek	90
5	1917	94.9	0.0	none	90
6	1947	94.9	1.0	Steep Gulch	90
7	2463	95.9	0.0	none	90
8	2493	95.9	12.6	Big Hollow	90
9	2604	108	0.0	none	90
10	3033	108	2.0	none	90
11	3063	110	5.9	Elephant Mountain Gulch	90
12	4182	116	5.4	none	90
13	4212	122	7.6	Palmer Gulch	90
14	4926	129	3.5	none	90

15	4956	133	9.2	Austin Gulch	90
16	5897	142	8.5	none	90
17	5927	151	5.9	Whitney Gulch	90
18	6091	156	1.5	none	90
19	6121	158	2.9	Smallpox Gulch	90
20	6344	161	2.0	none	90
21	6374	163	0.1	Moss Gulch	90
22	7770	163	12.6	none	90
23	7970	176	493	Upper Alamosa River	90
24	9269	668	59.2	none	90
25	9329	727	17.2	Fall Gulch	92
26	10640	745	59.7	none	92
27	10700	804	4.4	Cornwall Creek	92
28	11096	809	18.1	Dry Gulch	92
29	12713	827	39.2	Donkey Gulch	92
30	12773	866	21.0	Jasper Creek	92
31	13387	887	14.9	none	93
32	13447	902	9.1	Burnt Creek	93
33	13507	911	11.4	Brewer Creek	93
34	14549	922	25.3	none	93
35	14609	948	4.0	Spring Creek	93
36	15470	952	20.9	none	95
37	15530	972	3.4	Fern Creek	95
38	16531	976	24.3	none	96
39	16591	1000	10.2	Castleman Gulch	96
40	18943	1010	57.0	none	95.5
41	19003	1067	15.0	California Gulch	96
42	19506	1082	24.1	none	96
43	19566	1107	8.3	Silver Creek	96
44	21815	1115	67.1	none	96
45	21875	1182	41.1	Rough Canyon	96
46	21910	1223	1.0	none	96
47	21970	1224	17.6	Beaver Creek	96
48	23066	1242	32.7	none	97
49	23126	1274	9.2	Lieutenant Creek	97
50	24395	1284	37.8	none	97
51	24455	1321	23.9	Ranger Creek	97
52	25079	1345	18.6	none	97
53	25394	1364	-5.1	none	98
54	25454	1359	20.3	French Creek, Gypsy Gulch	98
55	30330	1379	-79.4	ARm35.4	97.5
56	30530	1300	0.0	none	97.5

3.5.2 High-Flow Streamflow Parameters

High-flow discharges from the tracer-injection synoptic study for the entire Wightman Fork-Alamosa River system are compared with measured discharges in figure 8. Alamosa River tributary discharges were used to distribute the observed mainstem flow increases, providing additional resolution (fig. 9). A close-up of the Wightman Fork discharge distribution is shown in figure 10. Model reaches, streamflows, and Fe(II) percentages used as high-flow model input are presented in Table 5.

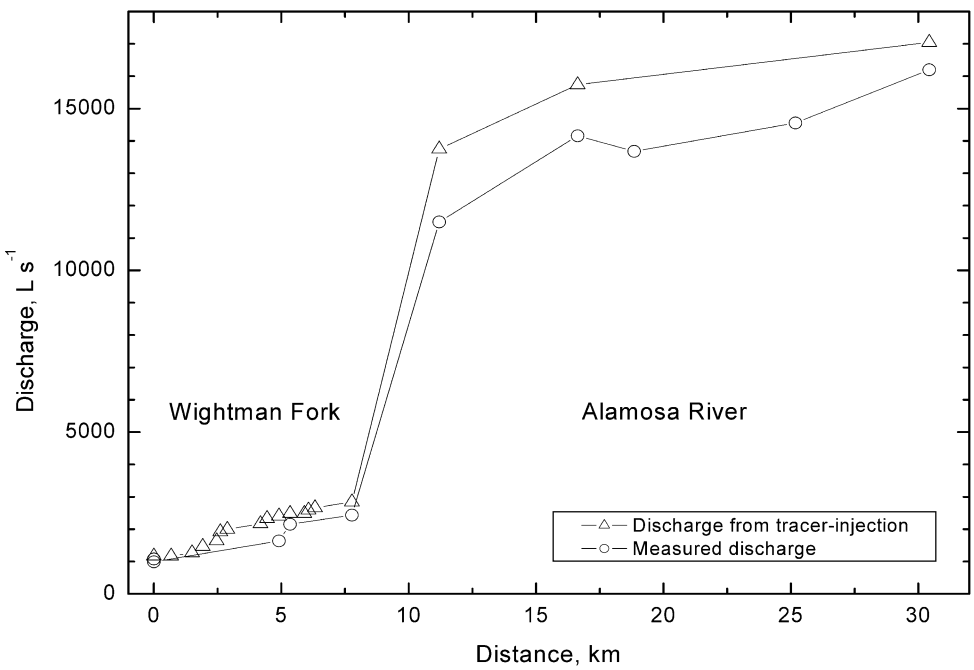

Figure 8. Comparison of high-flow discharges from instantaneous measurements and from the tracer-injection study

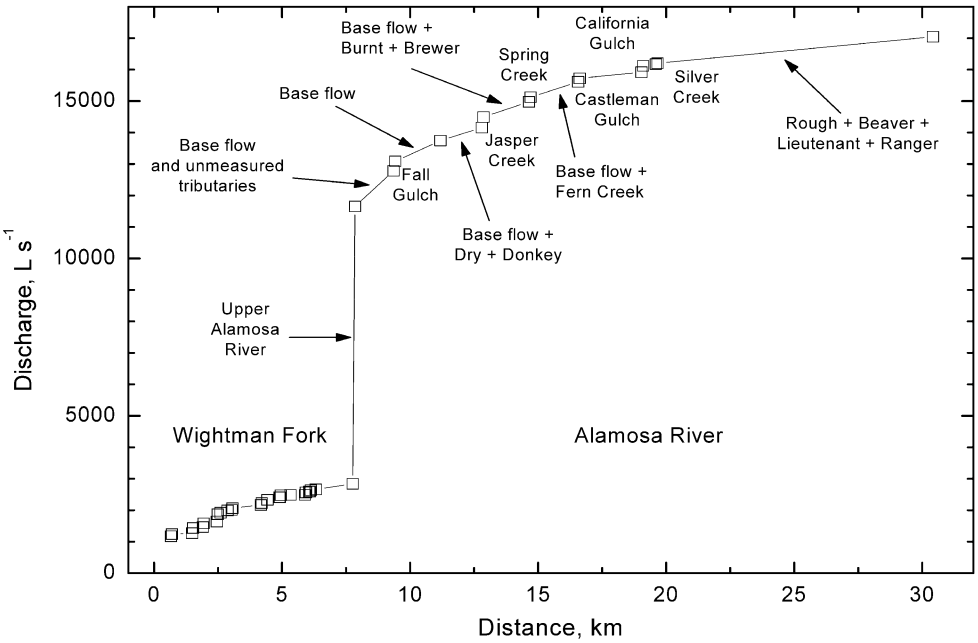

Figure 9. High-flow discharge distribution detail for the Alamosa River

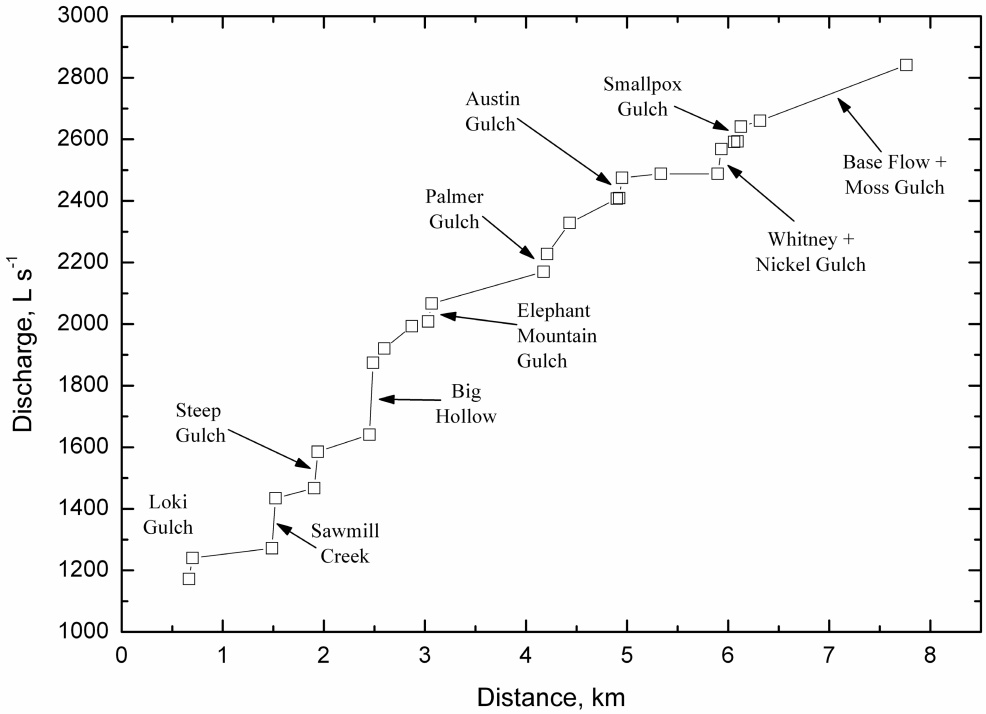

Figure 10. High-flow discharge distribution detail for Wightman Fork

Table 5. High-flow model reaches including streamflow, inflows, and Fe(II) percentages

Reach	Cumulative distance [m]	Stream flow [L s^{-1}] Top of reach	Within reach increase	Observed inflows	Fe(II) percentage
1	676	1172	10.2	Helokrene Gulch, Estival Gulch	60
2	706	1182	81.8	Loki Gulch	65
3	1497	1264	0.0	none	65
4	1527	1264	446	Sawmill Creek	70
5	1915	1710	0.0	none	75
6	1945	1710	142	Steep Gulch	80
7	2462	1852	0.0	none	85
8	2492	1852	279	Big Hollow	85
9	2607	2131	-211	none	85
10	2881	1920	1.7	Talus Spring, Greyback Mine	90
11	3042	1922	0.0	none	90
12	3072	1922	69.1	Elephant Mountain Gulch	90
13	4184	1991	0.0	none	95
14	4214	1991	68.2	Palmer Gulch	95
15	4442	2059	0.0	none	95
16	4909	2059	348	none	95
17	4926	2407	0.0	none	95
18	4956	2407	89.8	Austin Gulch	95
19	5344	2497	0.0	none	95
20	5907	2497	0.0	none	95
21	5937	2497	96.0	Whitney Gulch, Nickel Gulch	95
22	6068	2593	0.0	none	95
23	6100	2593	0.0	none	95
24	6130	2593	56.9	Smallpox Gulch	95
25	6325	2650	0.0	none	95
26	7773	2650	188	none	95
27	7853	2838	9401	Upper Alamosa River	99.1
28	9370	12239	0.0	none	95
29	9430	12239	326	Fall Gulch	95
30	11197	12565	149	none	95
31	12813	12714	0.0	Dry Gulch, Donkey Gulch	95
32	12873	12714	363	Jasper Creek	95
33	14650	13077	28.9	Burnt Creek, Brewer Creek	95
34	14710	13106	155	Spring Creek	95
35	16572	13261	777	Fern Creek	95
36	16632	14038	120	Castleman Gulch	95
37	19043	14158	-481	none	95
38	19103	13677	215	California Gulch	95
39	19607	13892	0.0	none	95
40	19667	13892	29.2	Silver Creek	95
41	30431	13921	36.8	Rough Canyon, Beaver Creek, Lieutenant Creek, Ranger Creek	95
42	30631	13958	2240	none	95

Inflow discharges from tracer-dilution calculations of the tracer-injection data for Wightman Fork are compared with their measured counterparts in figure 11. Tracer-dilution inflows are shown as diamonds connected by a line, while gaged tributaries are shown as circles. In most cases, the inflow from tracer-dilution calculations exceeds the gaged tributary. Two exceptions are the discharges for Sawmill Creek and Austin Gulch. The Sawmill Creek measurement was probably poor (Ortiz and Ball, 2003b), and the discrepancy for Austin Gulch is negligible.

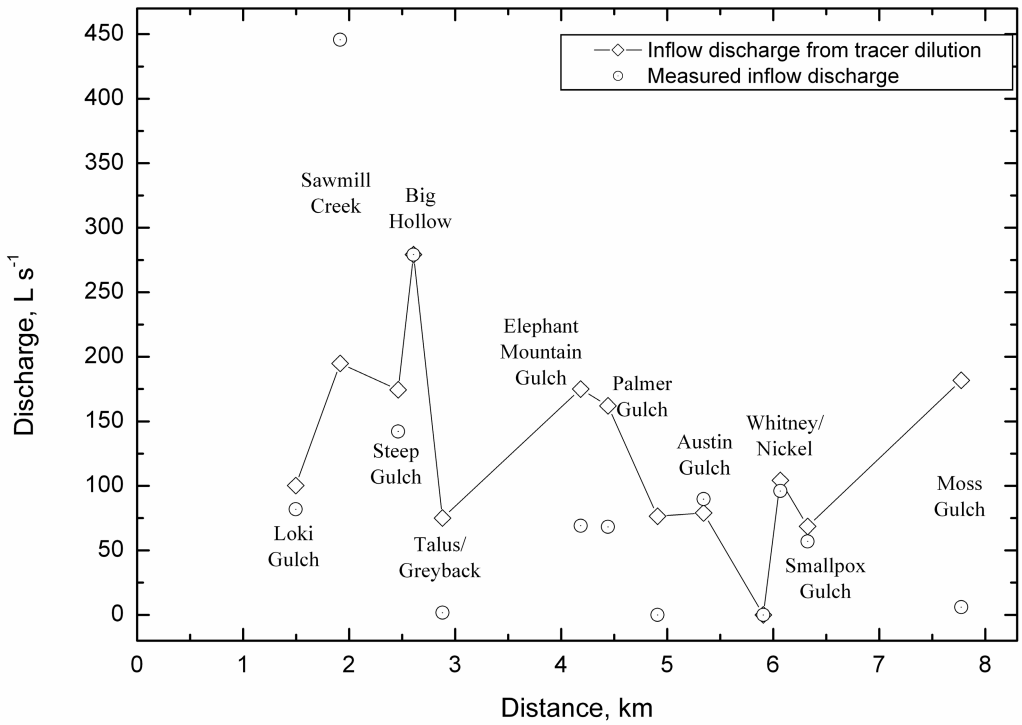

Figure 11. Comparison of high-flow inflow discharges from tracer-dilution and instantaneous measurements for Wightman Fork

In most cases, the calculated inflow exceeds the inflow measured at the tributary. This exceedance is to be expected as the dilution in each reach results from the sum of the tributary inflow and hyporheic flow.

3.6 Upstream Boundary Conditions

Upstream boundary conditions were set to the respective measured dissolved SO_4, Fe(II), Ca, Mg, F, and Mn and total recoverable Al, Fe(III), Cu, and Zn concentrations in Wightman Fork at WFm4.8. Values for H_T^+ and TIC were obtained by separate simulation using program MINTEQA2. Values for total recoverable Fe(III) were obtained as described in section 3.3. Upstream boundary condition concentrations used for the final model calibration runs for low and high flow are listed in Table 6.

Table 6. Upstream boundary condition concentrations at WFm4.8

Component	Low Flow	High Flow
	moles L^{-1}	
Dissolved		
SO_4	1.385E-02	2.291E-03
Fe(II)	3.706E-05	7.188E-05
Ca	1.146E-02	1.293E-03
Mg	1.146E-03	2.905E-04
F	3.737E-05	8.425E-06
Mn	8.976E-05	4.024E-05
H_T^+	-4.900E-04	-1.290E-04
TIC	1.067E-05	1.041E-05
Total recoverable		
Al	4.818E-04	2.866E-04
Fe(III)	1.845E-05	1.466E-04
Cu	2.093E-05	2.235E-05
Zn	1.492E-05	1.146E-05

At the upstream boundary the mass of sorbent within the water column was based on the amount of precipitated Fe(III), as determined by total recoverable Fe determinations and separate MINTEQA2 calculations. Wightman Fork water at the upstream boundary (WFm4.8) contained suspended material that was thought to be mostly hydrous ferric oxide (HFO). In order to include this suspended material in the OTEQ simulations it was necessary to create an upstream boundary condition that had both the selected simulation pH and the appropriate amount of suspended HFO. This was done by a separate MINTEQA2 simulation in which the equilibrium solution was modified by changing the metal concentrations to their total recoverable values. The input H_T^+ was varied and MINTEQA2 was run repeatedly to calculate the pH under these conditions until the correct pH and amount of precipitation of Fe and Al phases were simulated. When this was achieved the H_T^+ and the total recoverable Fe and Al concentrations were used in the OTEQ upstream boundary condition.

3.7 Geochemical Parameters

Temperature and ionic strength are spatially invariant within OTEQ. Therefore, because nearly all chemical reactions in the reach are nearly complete at the confluence of Wightman Fork and the Alamosa River, the temperature and ionic strength observed at stations WFm4.8 and WF0.0 were used to set these two parameters to 8°C and 0.03 molal for low flow and 4°C and 0.04 molal for high flow.

3.7.1 Thermodynamic Data

The thermodynamic data base for aqueous complexes and ion activity product calculations was that of MINTEQA2 (Allison et al., 1991) modified using the data from Nordstrom et al. (1990). Additional improvements and error corrections were made to the data base based on the simulation results of this paper.

Sorbent concentrations were based on the simulated concentration of precipitated Fe in each stream segment. The sorption data base was that of Dzombak and Morel (1990). Initial simulations using the best estimates of Dzombak and Morel resulted in underprediction of Cu sorption. The high affinity site density was therefore increased to the upper value reported by Dzombak and Morel to reflect the high sorptive capacity of freshly precipitated iron oxides (Runkel et al., 1999; Runkel and Kimball, 2002).

Investigations of white aluminous precipitates in acid mine waters indicate that this material can be approximated most closely by either crystalline to microcrystalline gibbsite [$Al(OH)_3$] or amorphous basaluminite [$Al_4(OH)_{10}SO_4$] (Nordstrom et al. 1984, Nordstrom 1982, Adams and Rawajfih 1977, Singh and Brydon 1970, Singh 1969). The following three reactions were used to define the precipitating phases for the OTEQ simulations:

$$Fe^{3+} + 3H_2O = Fe(OH)_3 + 3H^+, \quad (8)$$

$$Al^{3+} + 3H_2O = Al(OH)_3 + 3H^+, \quad (9)$$

and

$$4Al^{3+} + SO_4^{2-} + 10H_2O = Al_4(OH)_{10}SO_4 + 10H^+. \quad (10)$$

The respective MINTEQA2 default log K^o values of -4.891 and -8.77 for the solubility equilibrium constants for ferrihydrite and microcrystalline gibbsite solubility were used in the simulations. A log K^o value for basaluminite of -26.3 was estimated based on MINTEQA2 simulations. Ferrihydrite and basaluminite were used as the respective Al and Fe precipitating phases for the low-flow simulations and ferrihydrite and microcrystalline gibbsite were used as the respective Al and Fe precipitating phases for the high-flow simulations.

3.7.2 Reduction-Oxidation Parameters for Iron

Iron(II) was simulated to oxidize concurrently with Fe(III) hydrolysis and precipitation to achieve a ratio of dissolved Fe(II) to dissolved Fe(III) consistent with measured values of dissolved Fe(II) and Fe(III) at several locations in the main stem of Wightman Fork. The Fe(II)/Fe(total) ratio, discussed in section 3.3, was fixed to approximate the observed dissolved Fe(II) and Fe(III) concentrations measured for the main stem at the end of each modeled reach. The relations between observed Fe(II)/Fe(total) ratios and those specified in the OTEQ input are shown in figure 12 for low flow, and in figure 13 for high flow.

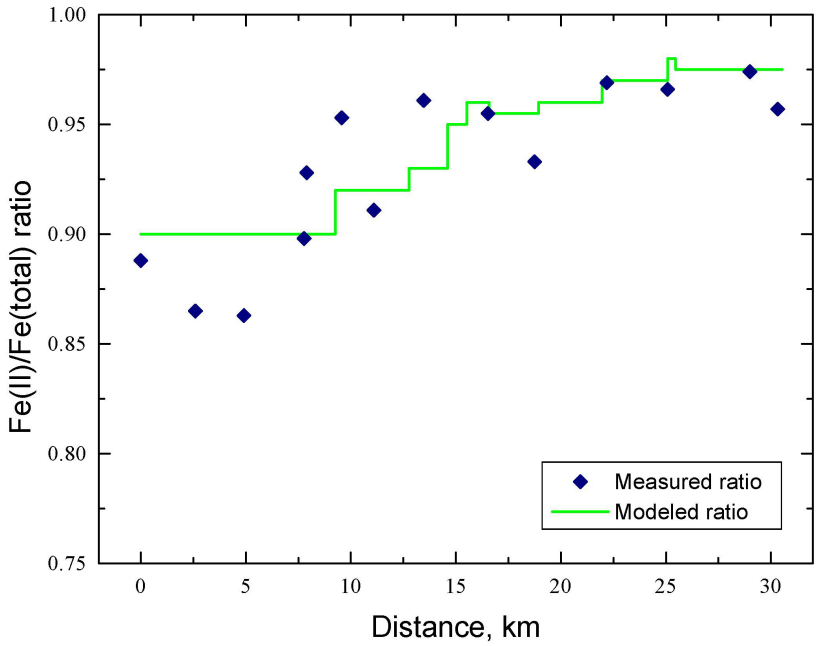

Figure 12. Observed dissolved Fe(II)/Fe(total) ratios compared with ratios used by the OTEQ model for the low-flow simulations.

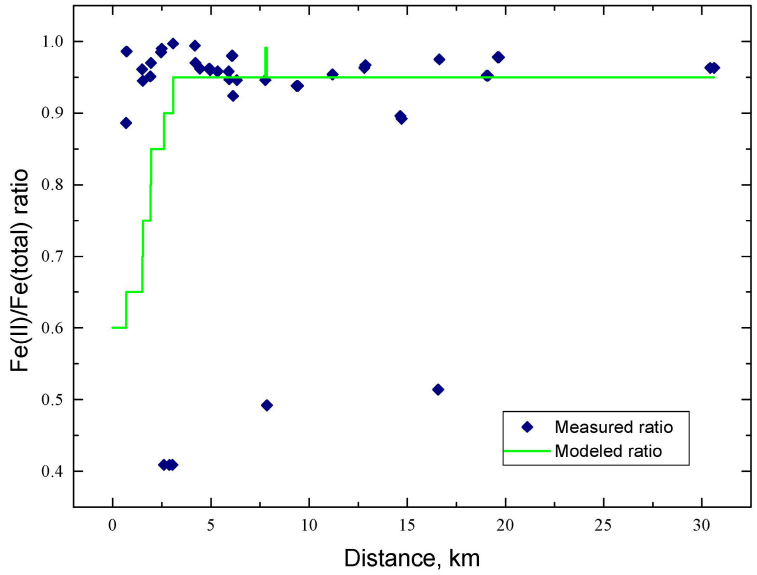

Figure 13. Observed dissolved Fe(II)/Fe(total) ratios compared with ratios used by OTEQ model for the high-flow simulations.

4 Results

4.1 Low-Flow Simulations

Simulation results for pH, Al, Fe, and Cu as a function of distance are shown in figures 14a-d. Figure 15 illustrates the conservative simulation of SO_4. The simulations reproduced observed data well for all components. The most notable feature (fig. 14) is the marked inflection at the confluence of Wightman Fork and the Alamosa River (WF0.0). Water from the upper Alamosa River introduces a considerable load of Fe and H ions (figs. 14a and c), whereas it dilutes the concentrations of Al and Cu (figs. 14b and d).

Inflow SO_4, Ca, and Mg concentration estimates were used to calculate discharges for Wightman Fork and its tributaries using the confluence mass-balance approach discussed in section 3.5.1. The model simulates the observed SO_4 (fig. 15), Ca, and Mg (data not shown) concentrations in Wightman Fork well, demonstrating that mass balance was maintained after adjustment of the discharges.

During preliminary simulation runs (Ball et al. 1999) water quality data for many tributaries were lacking. Therefore initial values were based on pH, alkalinity, and SO_4 of typical alpine stream water. Simulation results indicated that the initial tributary pH values and alkalinity and SO_4 concentrations did not reproduce values observed in Wightman Fork and the Alamosa River. Many of the pH values of about 8 and the high alkalinity concentrations that yielded sucessful model runs were later confirmed in field samples, illustrating the usefulness of reactive transport modeling as a tool to guide field investigations.

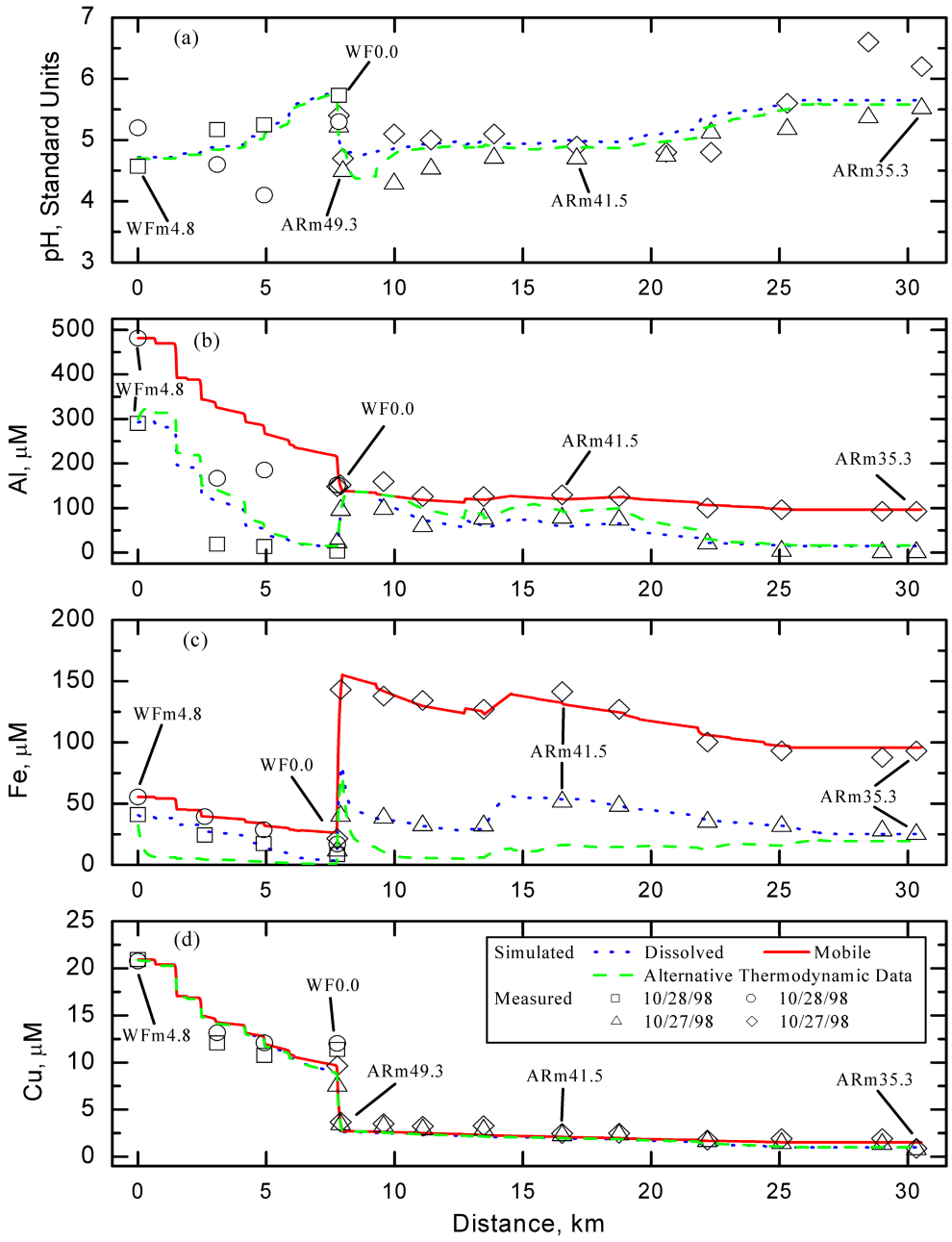

Figure 14. Low-flow OTEQ simulations of pH and Al, Fe, and Cu concentrations [for graph (a): □, field, or ○, laboratory, measured on 10/28/98; ◇, field, or △, laboratory, measured on 10/27/98; ·····, pH simulation using default thermodynamic data; - - - -, pH simulation using alternative thermodynamic data for aqueous $Fe(OH)_2^+$; for graphs (b), (c), and (d): Mobile, dissolved plus suspended (total recoverable); explanation in graph (d) also applies to graphs (b) and (c)]

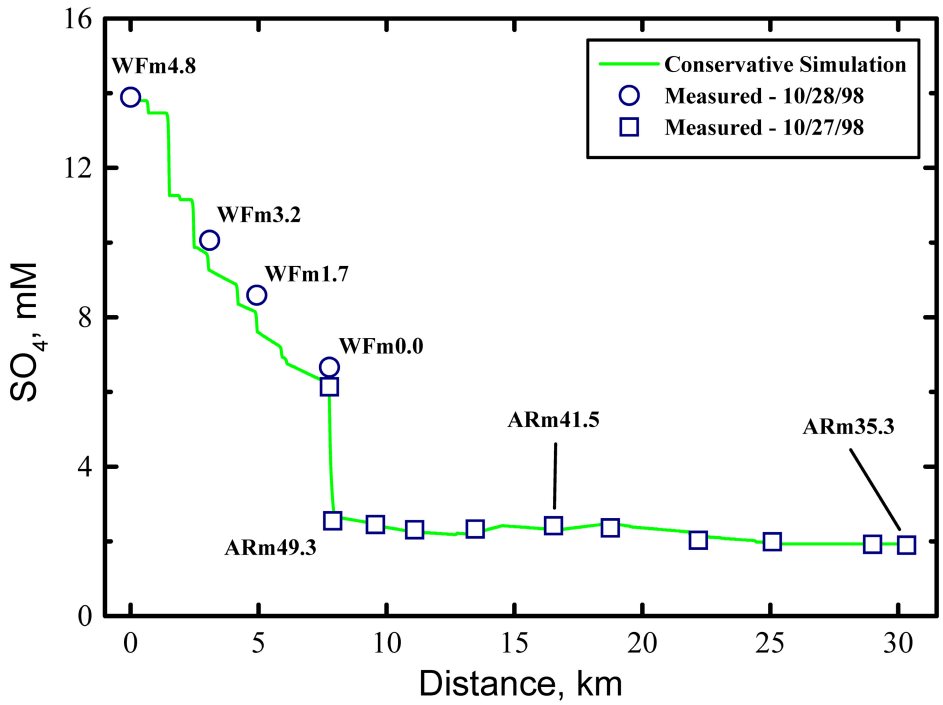

Figure 15. Low-flow conservative simulation of dissolved SO_4

Using tributary inflows with measured pH values and alkalinities derived using equilibrium with atmospheric CO_2, the reactive simulation of pH from Wightman Fork downstream from its confluence with Cropsy Creek to upstream from its confluence with the Alamosa River predicts the downstream pH in Wightman Fork well, despite the scatter in the field pH measurements (fig. 14a).

For the reactive Al simulation (fig. 14b), when microcrystalline gibbsite was used as the controlling phase for Al, the dissolved Al concentration was overpredicted at WFm3.2 (2.6 km, fig. 14b). Holding times prior to filtration for the WFm3.2 and WFm1.7 samples were on the order of several hours. Thus, hydrolysis and precipitation of dissolved Al may have occurred prior to sample filtration. Several combinations of solids, initial pH values, and K_{sp} values for the solids were used in simulations; however some initial precipitation of solids was calculated in every case.

4.2 High-Flow Simulations

Conservative and reactive simulation results for pH, and reactive simulation results for Al, Fe, and Cu, are shown in figures 16a-d. The contrast between low- and high-flow water chemistry is evident when comparing figures 14 and 16. Whereas at low flow H and Fe concentrations contributed by the upper Alamosa River were greater than those in Wightman

Fork, at high flow all dissolved and suspended components contributed by Wightman Fork were diluted by upper Alamosa River water.

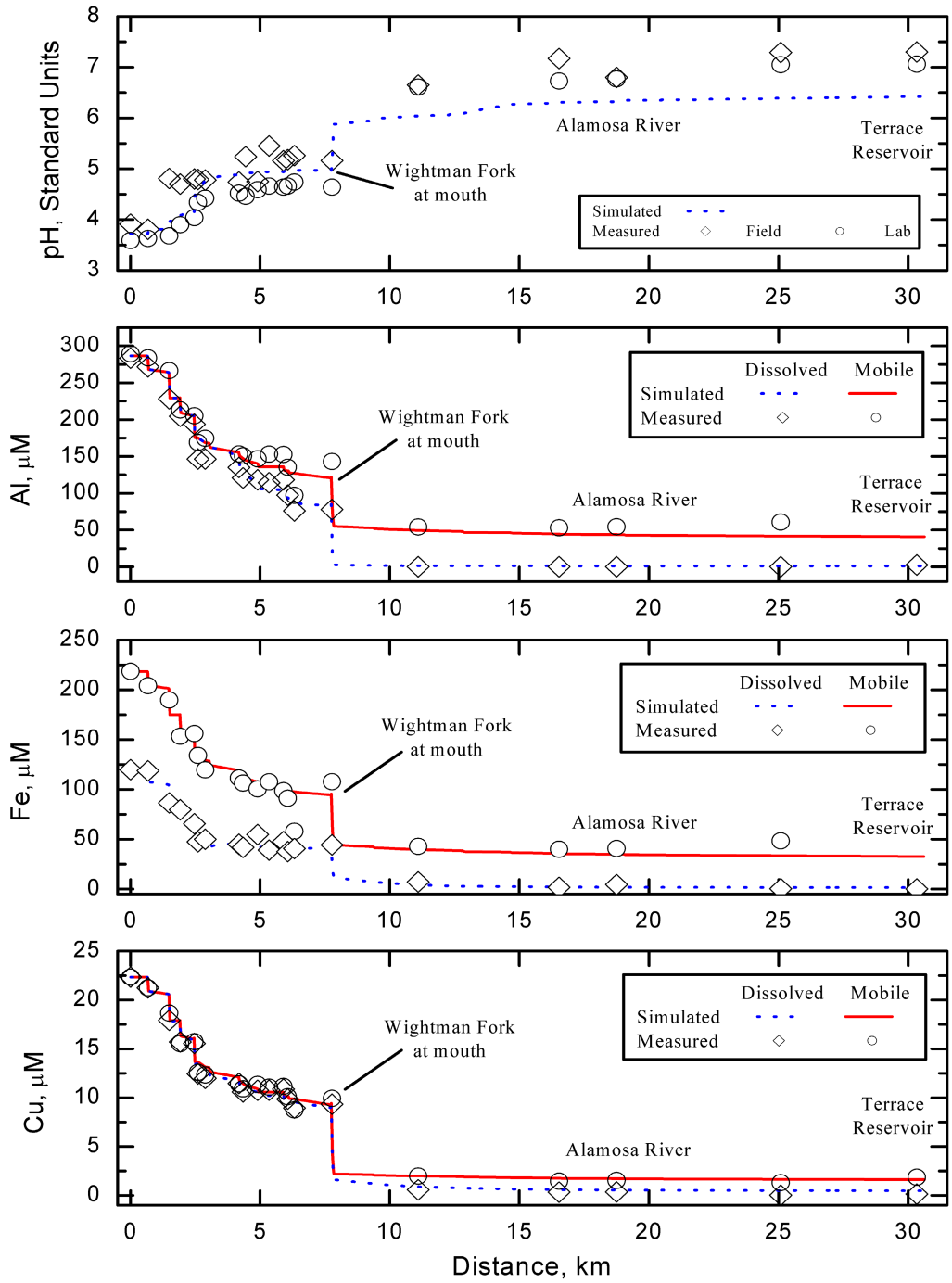

Figure 16. High-flow OTEQ simulations of pH and Al, Fe, and Cu concentrations

4.3 Thermodynamic Data and Sensitivity Analyses

Several of the OTEQ thermodynamic values used for the simulations discussed in this paper were markedly different from data used in the WATEQ4F chemical speciation program (Ball and Nordstrom, 1991). These data, together with mineral phase data relevant to this paper, are presented in Table 7. Several sensitivity analysis runs of OTEQ were made, varying one thermodynamic value at a time, and comparing the results to those obtained using the original MINTEQA2 data base. There was only one case, $\Delta_r H°$ for the aqueous ferric dihydroxide [$Fe(OH)_2^+$] species at low flow, where the alternative $\Delta_r H°$ makes a noticeable difference in simulation results. This result is an example of the potential for simulations to be sensitive to a single thermodynamic value. In this case, when the enthalpy is increased, more Fe^{3+} is hydrolyzed resulting in decreased pH, more dissolved Al, and less dissolved Fe (Fig. 14). Of note is that, despite the differences in simulated pH, Al, and Fe, the simulation of Cu sorption to hydrous ferric oxide is not appreciably changed. There were no appreciable differences in the high-flow simulation.

Table 7. Selected thermodynamic data used for OTEQ speciation and precipitation/dissolution simulations, including reactions where WATEQ4F and OTEQ differ markedly

Reaction	$\Delta_r H°$		Log K°	
Aqueous Species	WATEQ4F	OTEQ	WATEQ4F	OTEQ
$Al^{3+} + 2H_2O = Al(OH)_2^+ + 2H^+$	26.9	0	-10.1	-10.1
$Al^{3+} + 3H_2O = Al(OH)_3° + 3H^+$	39.89	0	-16.9	-16
$Al^{3+} + 2F^- = AlF_2^+$	1.98	20	12.7	12.75
$Fe^{3+} + SO_4^{2-} = FeSO_4^+$	3.91	3.91	4.04	3.92
$Fe^{3+} + 2H_2O = Fe(OH)_2^+ + 2H^+$	17.1	0	-5.67	-5.67
$Fe^{3+} + 3H_2O = Fe(OH)_3° + 3H^+$	24.8	0	-12.56	-13.6
$Fe^{3+} + 4H_2O = Fe(OH)_4^- + 4H^+$	31.9	0	-21.6	-21.6
Minerals				
$Fe^{3+} + 3H_2O = Fe(OH)_3 + 3H^+$	---	---	-4.891	-4.891
$Al^{3+} + 3H_2O = Al(OH)_3$ (μcryst) $+ 3H^+$	24.5	22.8	-9.35	-8.77
$4Al^{3+} + SO_4^{2-} + 10H_2O = Al_4(OH)_{10}SO_4 + 10H^+$	---	---	-22.8	-26.3

4.4 Summary of Model Calibrations

OTEQ simulations reproduce the general behavior of all components in the two stream segments of the study area. The fit to observed data supports the adequacy of the steady-state assumption for consideration of remediation options. Simulations indicate that Al, Cu, Fe, and H were reactive along the modeled segments, and that other solutes, including Ca, F, Mg, Mn, SO_4, and Zn, were non-reactive. The Cu results (figs. 14 and 16) demonstrate that sorption to the amount of Fe hydroxide precipitate actively forming in the water column quantitatively represents the observed data. Iron, Al, and Cu simulation results demonstrate

that the reactive behavior of these rapidly changing solutes can be simulated with good precision (figs. 14 - 16).

In this paper accurate simulation results are demonstrated using only measured dissolved and total recoverable concentrations of Fe and Cu. This represents a significant simulation result, because in reactive transport modeling the mass of sorbent in the water column frequently is considered an adjustable parameter. Zinc sorption (data not shown) was not demonstrated with certainty because Zn concentrations were so close to method detection limits that differences between dissolved and total Zn could not be measured with good precision.

Because of the high discharge of the Alamosa River relative to Wightman Fork, dissolved and suspended loads originating in the Alamosa River above Wightman Fork will be the determining factor in loading of the Alamosa River between Wightman Fork and Terrace Reservoir. When tributary chemical compositions with measured pH values and alkalinities derived using equilibrium with atmospheric CO_2 were used, the reactive simulation of pH from Wightman Fork below the Summitville Mine to the Alamosa River above Terrace Reservoir underpredicts the downstream pH. Titration alkalinities may be consistently underestimated with respect to measured pH values. Whereas pH is measured in situ, samples typically are filtered and titrated after Fe oxidation, and hydrolysis of Fe and Al, may have consumed a substantial fraction of the alkalinity. Unmeasured sources of neutralizing capacity also may be causing measured pH values to be higher than simulated values.

5 Remediation

Five remediation scenarios were simulated, by adjusting the flow and concentrations at the upstream boundary of the modeled system. The five remediation scenarios were:

1. No further action. Breach the holding pond and discontinue water treatment.
2. Discontinue water treatment. Divert clean water around the mine site and increase the holding pond capacity. Water in the holding pond to be metered out to Wightman Fork over a 6-month period each year.
3. Structurally upgrade the existing holding pond to meet Colorado State dam requirements, and construct a new water treatment plant to be operated seasonally.
4. Structurally upgrade the existing holding pond to meet Colorado State dam requirements. Retain the existing water treatment plant and keep it on line.
5. Construct a new holding pond upstream from Cropsy Creek and a new, expanded water treatment plant.

No remediation standards have been established for Wightman Fork between the Summitville Mine and its confluence with the Alamosa River. Variations of the five remediation scenarios described above also were simulated. At low flow, changes in water flow and chemistry of the upper Alamosa River above its confluence with Wightman Fork that might result from an intense summer rainstorm were calculated and input to OTEQ at the upper Alamosa River model reach (number 23, fig. 5) for scenario 5 (5 AR Rain). Also at

low flow, OTEQ simulations for scenarios 3, 4, and 5 were run with upstream boundary condition inputs for Wightman Fork that reflected flow and chemistry calculated with the Summitville water treatment plant (WTP) taken offline, such as for routine maintenance or due to a malfunction (3 WTP off, 4 WTP off, 5 WTP off). Selected upstream boundary conditions for Wightman Fork and upper Alamosa River inflow concentrations for the five scenarios and their variations are presented in Tables 8 and 9.

Table 8. Upstream boundary condition concentrations for Wightman Fork at WFm4.8 used for remediation alternatives 1 to 3 [WTP, water treatment plant]

	Scenario 1		Scenario 2		Scenario 3		
	Low Flow	High Flow	Low Flow	High Flow	Low Flow		High Flow
					WTP on	WTP off	
Component	moles L^{-1}		moles L^{-1}		moles L^{-1}		
SO_4	4.988E-03	2.721E-03	8.370E-03	2.086E-03	1.598E-02	3.892E-03	3.327E-03
Fe(II)	1.407E-03	4.867E-05	7.939E-04	5.829E-05	4.150E-05	9.462E-05	2.213E-05
Ca	2.452E-03	9.710E-04	2.928E-03	8.842E-04	1.226E-02	1.558E-03	1.881E-03
Mg	9.743E-04	3.345E-04	9.837E-04	3.081E-04	1.145E-03	5.066E-04	3.634E-04
F	3.737E-05	8.425E-06	3.737E-05	8.425E-06	3.737E-05	3.737E-05	8.425E-06
Mn	1.786E-04	8.696E-05	2.241E-04	7.161E-05	9.186E-05	7.372E-05	7.653E-05
Al	8.413E-03	8.680E-04	1.766E-03	4.660E-04	5.092E-04	1.058E-03	6.905E-04
Fe(III)	7.856E-04	4.480E-04	8.843E-05	2.308E-04	9.353E-05	2.124E-04	2.795E-04
Cu	2.470E-04	4.054E-05	1.902E-04	4.156E-05	1.550E-05	3.477E-05	1.731E-05
Zn	8.834E-05	2.369E-05	8.848E-05	2.162E-05	1.178E-05	2.677E-05	1.702E-05
H_T^+	-1.565E-03	-1.407E-03	2.416E-04	-5.626E-04	-7.400E-04	-1.500E-03	-1.884E-03
TIC	1.012E-05	1.050E-05	1.019E-05	1.028E-05	1.050E-05	1.037E-05	1.055E-05

Table 9. Upstream boundary condition concentrations for Wightman Fork at WFm4.8 and inflow concentrations for theupper Alamosa River used for remediation alternatives 4 and 5 [WTP, water treatment plant; AR, upper Alamosa River inflow]

	Scenario 4			Scenario 5		Scenario 5 Rain		Scenario 5
	Low Flow		High Flow	Low Flow		Low Flow, WTP on		High Flow
	WTP on	WTP off		WTP on	WTP off	WFm4.8	AR	
Component		moles L^{-1}				moles L^{-1}		
SO_4	1.723E-02	2.881E-03	2.551E-03	1.723E-02	2.843E-03	1.723E-02	1.283E-03	2.530E-03
Fe(II)	1.119E-05	3.838E-05	8.787E-06	1.199E-05	3.736E-05	1.199E-05	1.811E-04	7.937E-06
Ca	1.375E-02	1.743E-03	1.799E-03	1.376E-02	1.732E-03	1.376E-02	5.902E-04	1.792E-03
Mg	1.236E-03	5.236E-04	3.253E-04	1.236E-03	5.198E-04	1.236E-03	2.685E-04	3.230E-04
F	3.737E-05	3.737E-05	8.425E-06	3.737E-05	3.737E-05	3.737E-05	6.843E-06	8.425E-06
Mn	9.033E-05	6.246E-05	6.888E-05	8.987E-05	6.102E-05	8.987E-05	1.342E-05	6.811E-05
Al	2.220E-04	4.475E-04	3.645E-04	2.195E-04	4.408E-04	2.195E-04	5.685E-04	3.608E-04
Fe(III)	9.049E-05	2.388E-04	2.695E-04	8.866E-05	2.369E-04	8.866E-05	1.583E-05	2.688E-04
Cu	5.923E-06	1.479E-05	6.997E-06	5.652E-06	1.404E-05	5.652E-06	7.554E-07	6.593E-06
Zn	4.566E-06	1.189E-05	9.13E-06	4.441E-06	1.155E-05	4.441E-06	1.535E-06	8.944E-06
H_T^+	-7.443E-04	-1.340E-03	-1.646E-03	-7.345E-04	-1.340E-03	-7.345E-04	-2.693E-04	-1.641E-03
TIC	1.530E-05	1.052E-05	1.078E-05	1.592E-05	1.053E-05	1.592E-05	1.366E-05	1.079E-05

Low-flow conditions are the most important for two reasons. First, Wightman Fork and the Alamosa River are only at high flow for a few weeks each year. Secondly, spring snowmelt runoff dilutes the metals and hydronium ions that are dissolved in the water of Wightman Fork. This results in reduced metal concentrations and increased pH.

Aquatic risk drivers for the Alamosa River were identified in the Summitville Mine Superfund Site Tier 2 Ecological Risk Assessment (Camp Dresser and McKee Federal Programs Corporation, 2000). An aquatic risk driver is a water-quality parameter that is likely to exceed the standard established for risk to aquatic receptors in a particular stream segment. The parameters for the reach of the Alamosa River under study were pH, dissolved Cu and Zn, and total recoverable Fe. Because the State of Colorado Surface Water Standards for Cu and Zn are a function of hardness (CDPHE, 1998), Ca and Mg also are important. There are five points along the Wightman Fork-Alamosa River drainage, termed evaluation locations, where these chemical components are important: 1) Wightman Fork downstream from Cropsy Creek (WFm4.8); 2) Wightman Fork immediately upstream from its confluence with the Alamosa River at the WF0.0 gaging station; 3) the Alamosa River downstream from its confluence with Wightman Fork, upstream from the town of Jasper near the ARm49.4 sampling site; 4) the Alamosa river downstream from its confluence with Fern Creek, downstream from the town of Jasper near the ARm44.0 sampling site; and 5) the Alamosa River upstream from Terrace Reservoir (ARm35.4). For these five locations, simulated metal concentrations and pH were compared with the target values for water-quality parameters for

chronic exposure presented in Table 10. Why the target concentration for Cu at ARm49.4 is a single value rather than a calculated table value standard, similar to Zn, is not explained by CDPHE (1998). Both stream segments are identically classified "Aquatic Life Cold 1," "Recreation 2," and "Agriculture" (CDPHE, 1998). Sample site ARm49.4 is included in stream segment 3b, but the discussion of this segment does not mention Cu.

Table 10. Target values for evaluation locations along Wightman Fork and the Alamosa River [Tot. Recov., total recoverable]

		Dissolved		Tot. Recov.
		Cu	Zn	Fe
Location	pH	moles L^{-1}		
WFm4.8	---[1]	---	---	---
WF0.0	---	---	---	---
ARm49.4	6.5-9.0	4.72E-07	TVS[2]	2.15E-04
ARm44.0	6.5-9.0	TVS[3]	TVS[2]	2.15E-04
ARm35.4	6.5-9.0	TVS[3]	TVS[2]	2.15E-04

[1]---, no standard specified for this reach

[2]Table Value Standard for Zn (CDPHE, 1998), calculated as follows (hardness in mg/L as $CaCO_3$):

Acute: $e^{(0.8473[\ln(hardness)]+0.8604)}$

Chronic: $e^{(0.8473[\ln(hardness)]+0.7614)}$

For the Alamosa River between Wightman Fork and Terrace Reservoir, the chronic toxicity target value is $(7.0\text{-}7.5)\times10^{-7}$ M.

[3]Table Value Standard for Cu (CDPHE, 1998), calculated as follows:

Acute: $e^{(0.9422[\ln(hardness)]-1.4634)}$

Chronic: $e^{(0.8545[\ln(hardness)]-1.465)}$

For the Alamosa River between Wightman Fork and Terrace Reservoir, the chronic toxicity target value is $(8.0\text{-}8.5)\times10^{-8}$ M.

Simulation results showing values of pH, concentrations of dissolved Cu, Zn, and Fe, and concentrations of total recoverable Fe are presented in Tables 11 through 20. Values in **bold** denote failure to meet the water-quality standard. Graphs comparing simulation results for the five remediation scenarios, including the variations for scenarios 3, 4, and 5, at the five locations for low and high flow are shown in figures 17 through 26.

Table 11. Values of pH and concentrations of low-flow aquatic risk drivers for Wightman Fork below the Summitville Mine Site (WFm4.8, 0 meters) [Tot. Recov., total recoverable; WTP, water treatment plant; AR, upper Alamosa River]

			Dissolved		Tot. Recov.
		Cu	Zn	Fe	Fe
Scenario	pH	moles L^{-1}			
1	3.44	2.468E-04	8.833E-05	1.533E-03	2.193E-03
2	3.62	1.903E-04	8.848E-05	8.824E-04	8.824E-04
3	4.72	1.528E-05	1.178E-05	4.414E-05	1.350E-04
3 WTP offline	4.50	3.417E-05	2.677E-05	8.622E-05	3.070E-04
4	5.87	3.888E-06	4.552E-06	1.036E-05	1.017E-04
4 WTP offline	4.78	1.391E-05	1.188E-05	3.841E-05	2.773E-04
5	5.87	3.724E-06	4.427E-06	1.106E-05	1.007E-04
5 AR Rain	5.87	3.724E-06	4.427E-06	1.106E-05	1.007E-04
5 WTP offline	4.79	1.317E-05	1.154E-05	3.744E-05	2.743E-04

Table 12. Values of pH and concentrations of low-flow aquatic risk drivers for Wightman Fork above the Alamosa River (WF0.0, 7774 meters) [Tot. Recov., total recoverable; WTP, water treatment plant; AR, upper Alamosa River]

			Dissolved		Tot. Recov.
		Cu	Zn	Fe	Fe
Scenario	pH	moles L^{-1}			
1	3.93	8.038E-05	2.873E-05	2.788E-04	7.139E-04
2	4.54	5.631E-05	2.641E-05	6.267E-05	2.642E-04
3	5.74	5.979E-06	5.308E-06	3.991E-06	6.149E-05
3 WTP offline	5.75	7.188E-06	6.900E-06	3.923E-06	8.000E-05
4	6.83	5.177E-07	2.309E-06	4.083E-07	5.255E-05
4 WTP offline	6.54	9.725E-07	3.197E-06	7.558E-07	7.432E-05
5	6.84	4.941E-07	2.249E-06	4.256E-07	5.187E-05
5 AR Rain	6.83	4.965E-07	2.272E-06	4.217E-07	5.191E-05
5 WTP offline	6.56	8.891E-07	3.071E-06	7.299E-07	7.347E-05

Table 13. Values of pH and concentrations of low-flow aquatic risk drivers for the Alamosa River below Wightman Fork (ARm49.4, 7970 meters) [Tot. Recov., total recoverable; WTP, water treatment plant; AR, upper Alamosa River]

		Dissolved			Tot. Recov.
		Cu	Zn	Fe	Fe
Scenario	pH	moles L^{-1}			
1	**4.14**	**2.421E-05**	**9.567E-06**	1.762E-04	**3.544E-04**
2	**4.37**	**1.673E-05**	**8.684E-06**	1.088E-04	**2.198E-04**
3	**4.89**	**2.517E-06**	**2.699E-06**	7.440E-05	1.536E-04
3 WTP offline	**4.88**	**2.634E-06**	**2.893E-06**	7.873E-05	1.673E-04
4	**5.08**	**1.251E-06**	**1.731E-06**	6.789E-05	1.468E-04
4 WTP offline	**4.98**	**1.296E-06**	**1.880E-06**	7.485E-05	1.655E-04
5	**5.08**	**1.207E-06**	**1.708E-06**	6.789E-05	1.466E-04
5 AR Rain	**4.66**	**1.545E-06**	**1.797E-06**	1.126E-04	1.498E-04
5 WTP offline	**4.98**	**1.244E-06**	**1.854E-06**	7.478E-05	1.653E-04

Table 14. Values of pH and concentrations of low-flow aquatic risk drivers for the Alamosa River below Fern Creek (ARm44.0, 15,538 meters) [Tot. Recov., total recoverable; WTP, water treatment plant; AR, upper Alamosa River]

		Dissolved			Tot. Recov.
		Cu	Zn	Fe	Fe
Scenario	pH	moles L^{-1}			
1	**4.56**	**1.261E-05**	**5.292E-06**	1.098E-04	**2.456E-04**
2	**4.78**	**8.649E-06**	**4.815E-06**	6.588E-05	1.762E-04
3	**4.94**	**1.606E-06**	**1.790E-06**	4.539E-05	1.427E-04
3 WTP offline	**4.93**	**1.625E-06**	**1.846E-06**	4.652E-05	1.492E-04
4	**5.01**	**9.651E-07**	**1.288E-06**	3.810E-05	1.394E-04
4 WTP offline	**4.98**	**9.612E-07**	**1.334E-06**	4.194E-05	1.483E-04
5	**5.01**	**9.406E-07**	**1.276E-06**	3.811E-05	1.392E-04
5 AR Rain	**4.69**	**1.224E-06**	**1.385E-06**	8.010E-05	1.425E-04
5 WTP offline	**4.98**	**9.351E-07**	**1.321E-06**	4.147E-05	1.482E-04

Table 15. Values of pH and concentrations of low-flow aquatic risk drivers for the Alamosa River above Terrace Reservoir (ARm35.4, 30,330 meters) [Tot. Recov., total recoverable; WTP, water treatment plant; AR, upper Alamosa River]

		Dissolved			Tot. Recov.
		Cu	Zn	Fe	Fe
Scenario	pH	moles L^{-1}			
1	**4.76**	**8.857E-06**	**3.760E-06**	1.332E-04	1.718E-04
2	**5.30**	**5.557E-06**	**3.418E-06**	4.853E-05	1.231E-04
3	**5.65**	**7.253E-07**	**1.313E-06**	2.926E-05	1.009E-04
3 WTP offline	**5.65**	**7.074E-07**	**1.336E-06**	2.978E-05	1.040E-04
4	**5.74**	**3.510E-07**	**9.613E-07**	2.639E-05	9.908E-05
4 WTP offline	**5.72**	**3.372E-07**	**9.774E-07**	2.774E-05	2.774E-05
5	**5.74**	**3.403E-07**	**9.524E-07**	2.641E-05	9.901E-05
5 AR Rain	**4.99**	**8.857E-07**	**1.064E-06**	8.167E-05	1.040E-04
5 WTP offline	**5.72**	**3.254E-07**	**9.681E-07**	2.770E-05	1.033E-04

Table 16. Values of pH and concentrations of high-flow aquatic risk drivers for Wightman Fork below the Summitville Mine Site (WFm4.8, 0 meters) [Tot. Recov., total recoverable]

		Dissolved			Tot. Recov.
		Cu	Zn	Fe	Fe
Scenario	pH	moles L^{-1}			
1	4.65	3.835E-05	2.367E-05	4.929E-05	4.966E-04
2	4.21	4.132E-05	2.162E-05	6.496E-05	2.891E-04
3	4.81	1.495E-05	1.656E-05	1.889E-05	3.199E-04
4	5.06	5.733E-06	9.107E-06	9.903E-06	2.783E-04
5	5.07	5.357E-06	8.921E-06	9.103E-06	2.767E-04

Table 17. Values of pH and concentrations of high-flow aquatic risk drivers for Wightman Fork above the Alamosa River (WF0.0, 7774 meters) [Tot. Recov., total recoverable]

		Dissolved			Tot. Recov.
		Cu	Zn	Fe	Fe
Scenario	pH	moles L^{-1}			
1	4.81	1.729E-05	1.065E-05	5.897E-05	2.249E-04
2	5.02	1.328E-05	7.262E-06	3.757E-05	1.000E-04
3	5.09	6.667E-06	7.591E-06	3.139E-05	1.484E-04
4	5.92	1.240E-06	3.984E-06	6.600E-06	1.235E-04
5	5.94	1.116E-06	3.900E-06	6.411E-06	1.227E-04

Table 18. Values of pH and concentrations of high-flow aquatic risk drivers for the Alamosa River below Wightman Fork (ARm49.4, 7970 meters) [Tot. Recov., total recoverable]

		Dissolved			Tot. Recov.
		Cu	Zn	Fe	Fe
Scenario	pH	moles L^{-1}			
1	**5.21**	**4.094E-06**	**2.727E-06**	1.823E-05	7.695E-05
2	**6.01**	**2.106E-06**	**1.652E-06**	9.922E-06	4.383E-05
3	**6.04**	**9.885E-07**	**1.982E-06**	9.583E-06	5.842E-05
4	**6.43**	**1.383E-07**	**1.035E-06**	3.623E-06	5.149E-05
5	**6.44**	**1.244E-07**	**1.013E-06**	3.578E-06	5.131E-05

Table 19. Values of pH and concentrations of high-flow aquatic risk drivers for the Alamosa River below Fern Creek (ARm44.0, 15,538 meters) [Tot. Recov., total recoverable]

		Dissolved			Tot. Recov.
		Cu	Zn	Fe	Fe
Scenario	pH	moles L^{-1}			
1	**6.20**	**1.716E-06**	**2.224E-06**	3.722E-06	6.244E-05
2	6.61	**8.774E-07**	**1.356E-06**	1.862E-06	3.564E-05
3	6.62	**3.145E-07**	**1.603E-06**	1.650E-06	4.762E-05
4	6.90	6.224E-08	8.092E-07	1.097E-06	4.200E-05
5	6.90	5.710E-08	7.895E-07	1.084E-06	4.185E-05

Table 20. Values of pH and concentrations of high-flow aquatic risk drivers for the Alamosa River above Terrace Reservoir (ARm35.4, 30,330 meters) [Tot. Recov., total recoverable]

		Dissolved			Tot. Recov.
		Cu	Zn	Fe	Fe
Scenario	pH	moles L^{-1}			
1	**6.42**	**1.165E-06**	**2.001E-06**	2.117E-06	5.640E-05
2	6.78	**6.990E-07**	**1.215E-06**	1.244E-06	3.212E-05
3	6.79	**2.382E-07**	**1.428E-06**	1.063E-06	4.305E-05
4	7.05	5.698E-08	7.022E-07	7.240E-07	3.794E-05
5	7.06	5.261E-08	6.843E-07	7.141E-07	3.781E-05

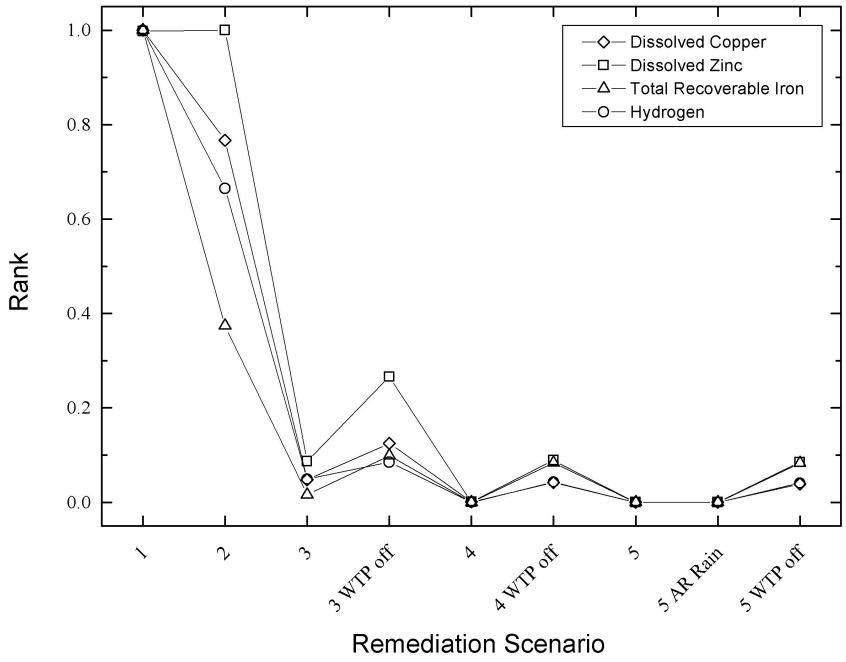

Figure 17. Ranking of the remediation scenario low-flow aquatic risk drivers for Wightman Fork below the Summitville Mine Site (WFm4.8, 0 meters)

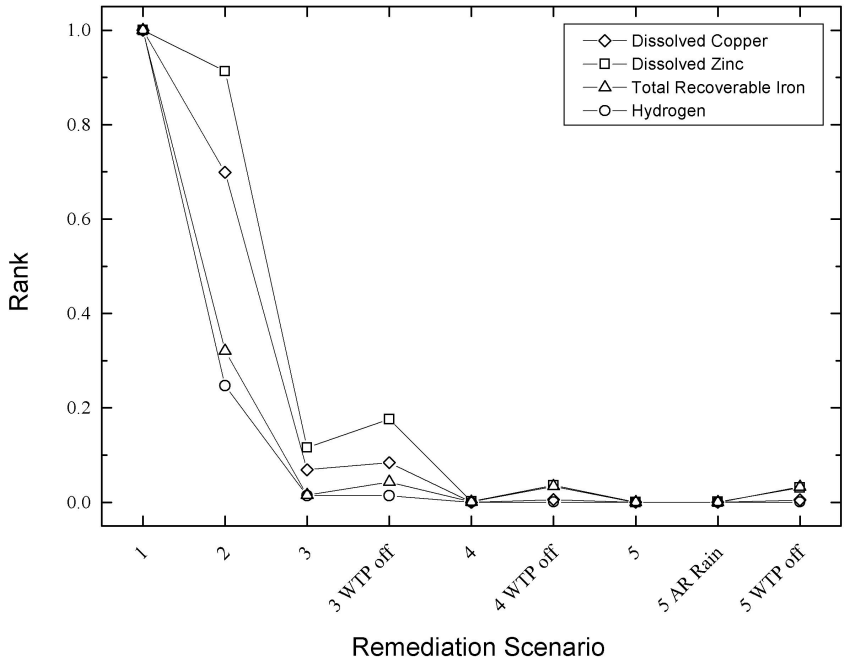

Figure 18. Ranking of the remediation scenario low-flow aquatic risk drivers for Wightman Fork above the Alamosa River (WF0.0, 7774 meters)

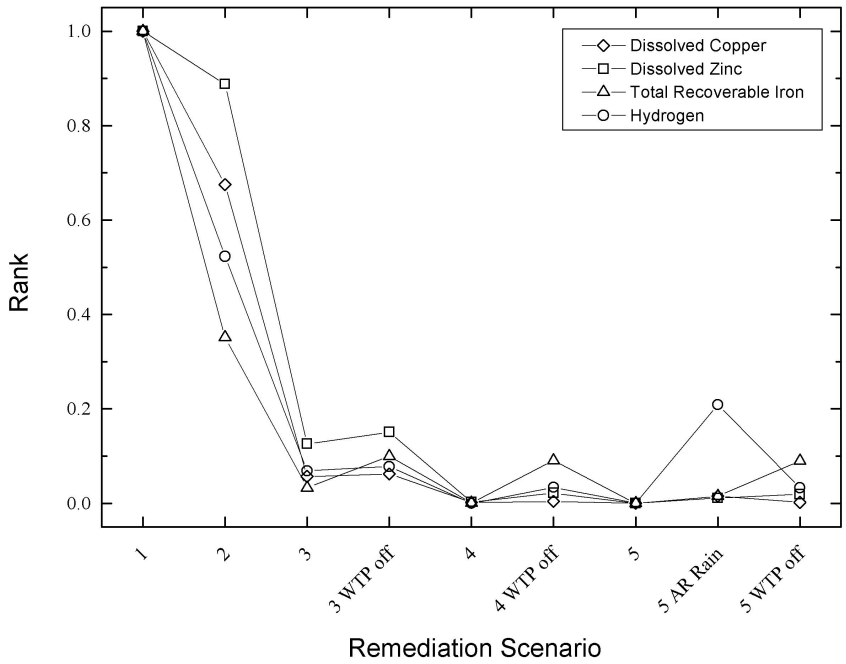

Figure 19. Ranking of the remediation scenario low-flow aquatic risk drivers for the Alamosa River below Wightman Fork (ARm49.4, 7970 meters)

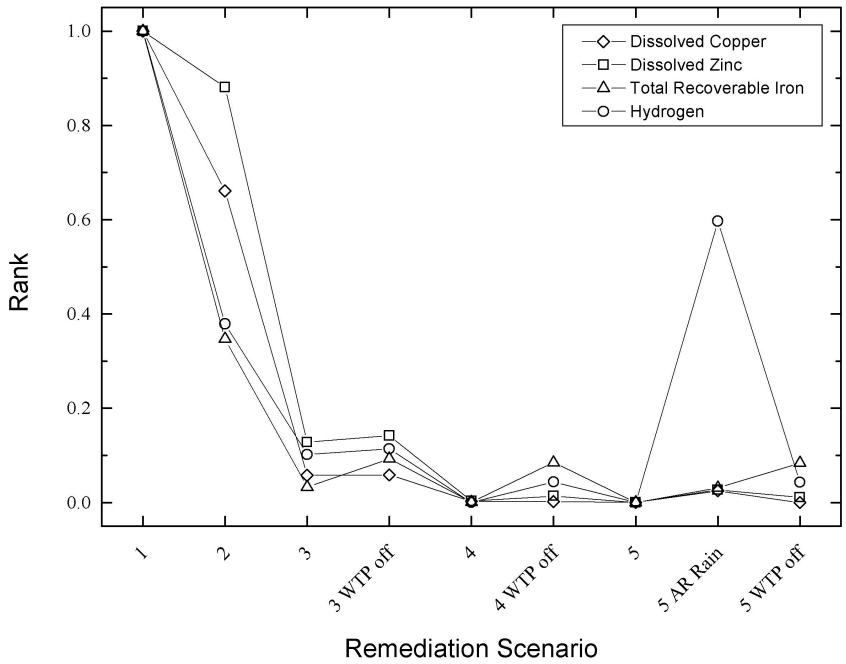

Figure 20. Ranking of the remediation scenario low-flow aquatic risk drivers for the Alamosa River below Fern Creek (ARm44.0, 15,538 meters)

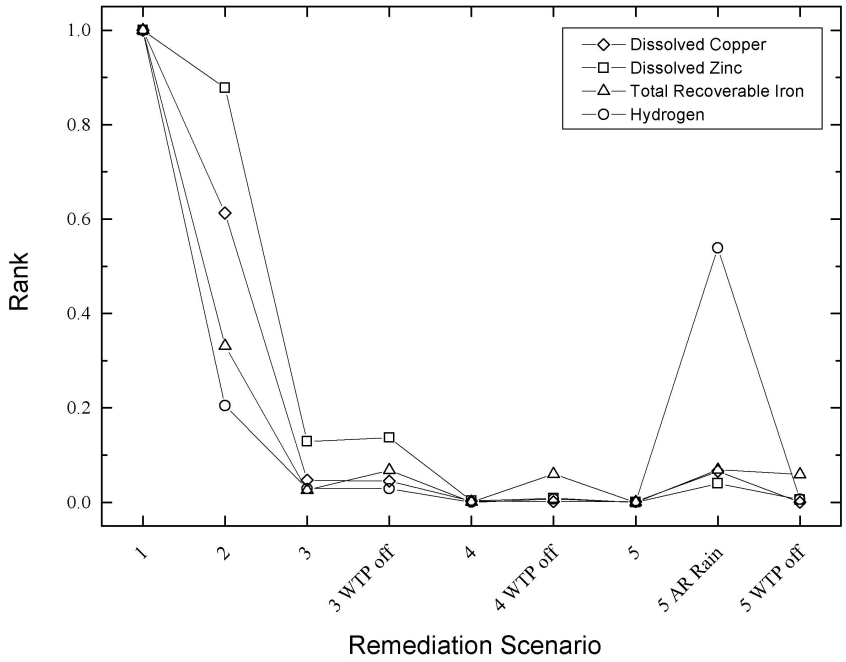

Figure 21. Ranking of the remediation scenario low-flow aquatic risk drivers for the Alamosa River above Terrace Reservoir (ARm35.4, 30,330 meters)

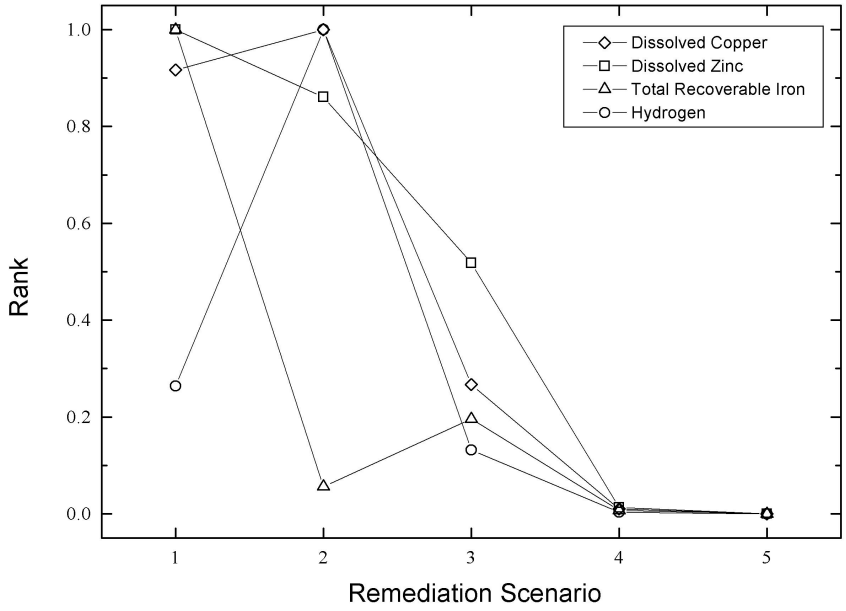

Figure 22. Ranking of the remediation scenario high-flow aquatic risk drivers for Wightman Fork below the Summitville Mine Site (WFm4.8, 0 meters)

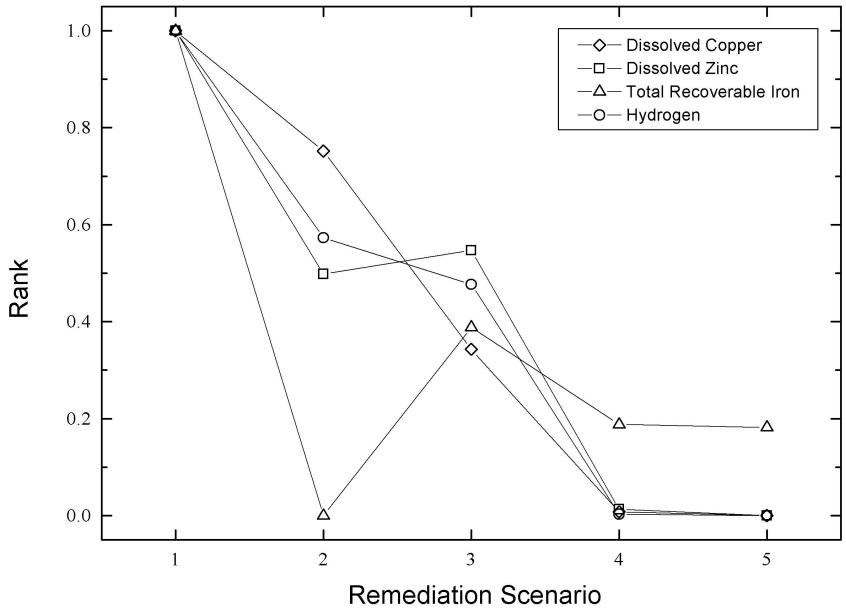

Figure 23. Ranking of the remediation scenario high-flow aquatic risk drivers for Wightman Fork above the Alamosa River (WF0.0, 7774 meters)

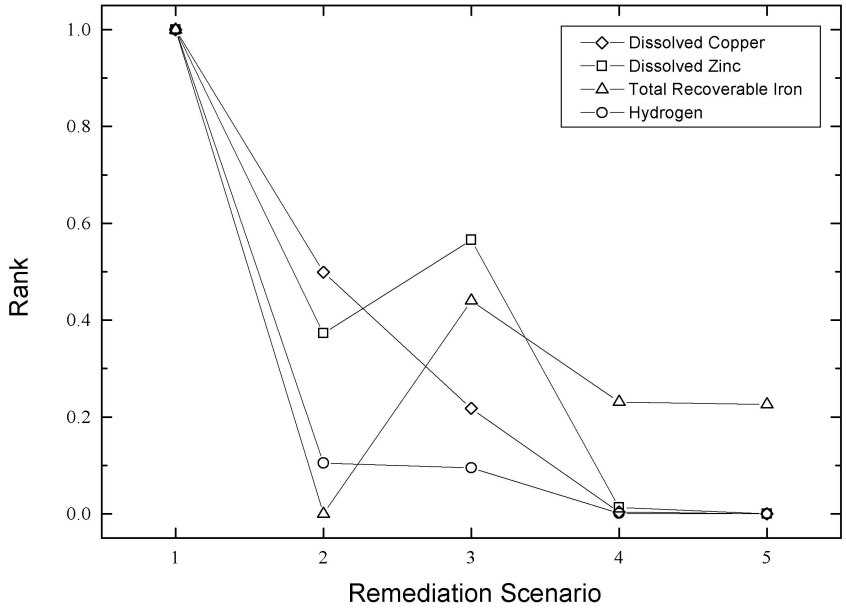

Figure 24. Ranking of the remediation scenario high-flow aquatic risk drivers for the Alamosa River below Wightman Fork (ARm49.4, 7970 meters)

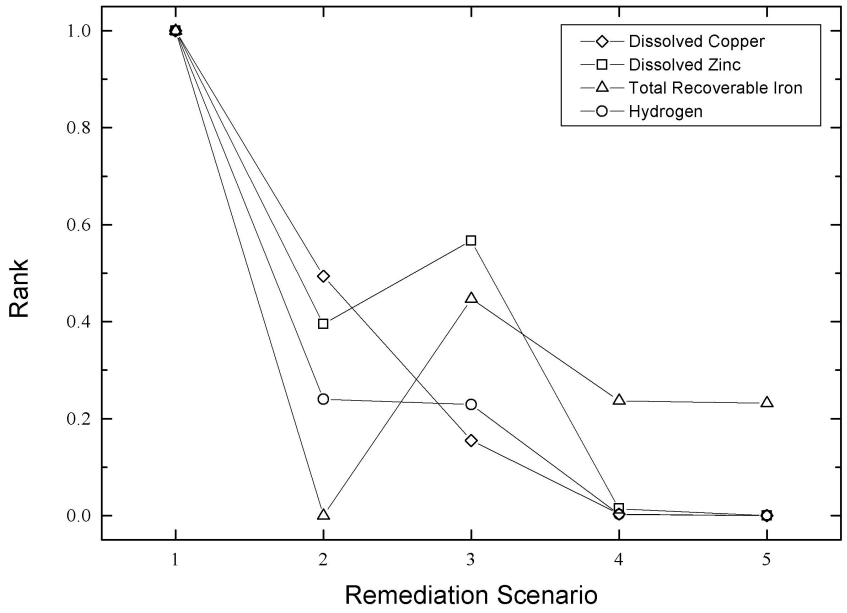

Figure 25. Ranking of the remediation scenario high-flow aquatic risk drivers for the Alamosa River below Fern Creek (ARm44.0, 15,538 meters)

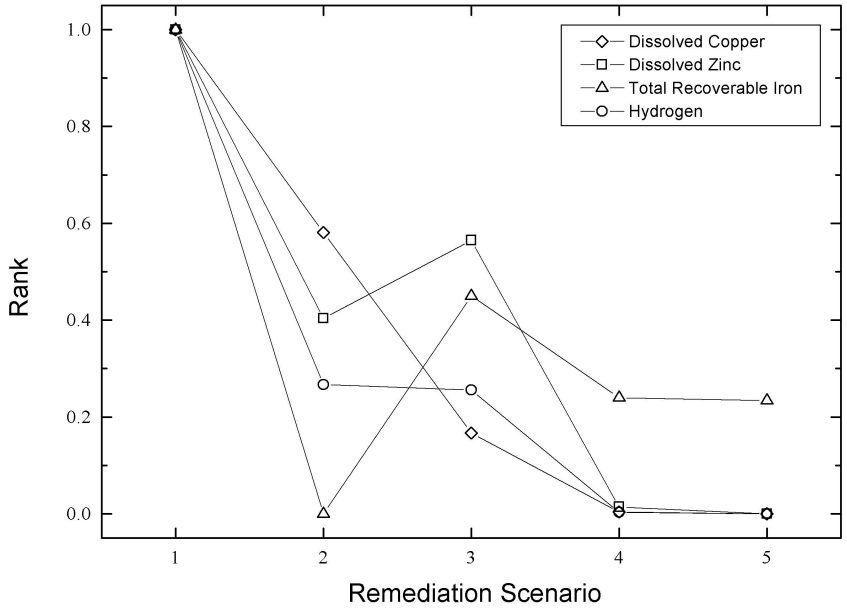

Figure 26. Ranking of the remediation scenario high-flow aquatic risk drivers for the Alamosa River above Terrace Reservoir (ARm35.4, 30,330 meters)

The ranks displayed in figs. 17-26 represent relative concentrations of the components and are calculated as follows:

$$\text{Rank} = \frac{C_i - C_{min}}{C_{max} - C_{min}} \qquad (11)$$

where C_i = concentration (M) of the component of interest for scenario i,
C_{min} = concentration (M) of the most dilute instance among all scenarios, and
C_{max} = concentration (M) of the most concentrated instance among all scenarios

The value of rank therefore can be between zero and 1, with 1 being the highest concentration, or most degraded water quality.

5.1 Low-Flow Remediation Scenarios

At low flow, target concentrations for Cu and Zn were exceeded (failed to meet the standard) for all tested scenarios in the Alamosa River. The target concentration for total recoverable Fe was exceeded for scenario 1 at ARm49.4 and ARm44.0, and was exceeded at ARm49.4 for scenario 2. The total recoverable Fe target concentration was met for scenarios 3-5, with or without the WTP online and with an upper Alamosa River rainstorm. Scenarios 1 and 2 yielded considerably poorer water quality than scenarios 3, 4, and 5. At WFm4.8 (fig. 17) there was little difference among scenarios 3, 4, and 5 with the WTP online. With the WTP taken offline, dissolved Zn for scenario 3 and dissolved Zn and total recoverable Fe for scenarios 4 and 5 were somewhat increased compared to their rankings with the WTP online. As expected, the rankings for WF0.0 (fig. 18) were not noticeably different from those for WFm4.8 (fig. 17).

For scenario 5, simulation of lateral inflow and chemistry for an intense rainstorm in the upper Alamosa River drainage basin generated a considerable spike of H^+ that was propagated through ARm49.4, ARm44.0 and ARm35.4 (figs. 19 to 21). Because the rainstorm was restricted to the upper Alamosa River drainage basin, its effect was not seen in the Wightman Fork drainage basin. Examination of the data in Tables 12-14 reveals that pH values for the rainstorm scenario (5 AR Rain) were the lowest for any of the scenario 3, 4, and 5 simulations, including those with the WTP offline. The reduction in pH occured because there was little buffering capacity in the Alamosa River from downstream of its confluence with Wightman Fork to Terrace Reservoir. Although not simulated for scenarios 3 and 4, a rainstorm in the upper Alamosa River drainage basin would be expected to have a similar effect on water quality.

5.2 High-Flow Remediation Scenarios

At high flow, total recoverable Fe met the standard for all tested scenarios at all three Alamosa River evaluation locations. Copper and Zn exceeded target concentrations (failed to meet the standard) for all tested scenarios at ARm49.4. At ARm44.0 and ARm35.4, the Cu and Zn standards were met for scenarios 4 and 5, but were exceeded for scenarios 1-3. Over

the entire length of the study area, there is little difference in water quality between scenarios 4 and 5, both of which would improve water quality considerably more than scenarios 1-3 (figs. 22-26). For scenario 3, there is only an incremental improvement in water quality over scenario 2 in Wightman Fork (Figs. 22 and 23), and there is little improvement in water quality in the Alamosa River (figs. 24-26). This is expected because the volume rate of flow during the spring snowmelt is so great that none of the treatment alternatives has the capability to handle the large discharges generated. However, the volume of snowmelt contributes significantly to dilution of contaminants and mitigates their effect. Thus, the remediation scenarios differ less at high flow than at low flow because of better natural water quality.

5.3 Evaluation of Remedial Alternatives

Among the remediation scenarios tested, implementation of remediation scenario 3 would result in water quality meeting target concentrations for some parameters. For more reliable reduction of the risk to aquatic life during high flow, scenario 4 appears preferable. Clearly, the alternative of doing nothing (remediation scenario 1) carries with it the greatest risk of damage to aquatic life in this segment of the Alamosa River. An intense rainstorm in the drainage area of the upper Alamosa River, for which no mitigation plans are anticipated, has the potential to substantially reduce the pH of the Alamosa River with possible chemical remobilization of Cu that has been sequestered by the hydrous ferric oxide precipitates in the stream channel. Thus, it appears unlikely under any scenario simulated in this study that absolute protection of aquatic life at all times can be achieved in the Alamosa River from its confluence with Wightman Fork to Terrace Reservoir.

Acknowledgments

The authors would like to acknowledge the collaboration and support of the Colorado Department of Public Health and Environment and the U.S. Environmental Protection Agency. The authors thank Doug Kent and Blaine McCleskey of the U.S. Geological Survey for many helpful comments and suggestions. We are expecially grateful to Rodger Ortiz of the U.S. Geological Survey, Pueblo District Office, for his significant contributions to the field operations and their descriptions that have been incorporated into this paper.

The use of firm, trade, and brand names in this paper is for identification purposes only and does not constitute endorsement by the U.S. Geological Survey.

References

Achterberg, E.P., C. Braungardt, N.H. Morley, F. Elbaz-Paulichert, and M. LeBlanc. 1999. Impact of Los Frailes mine spill on riverine, estuarine, and coastal waters in southern Spain. *Water Resources* **33**:3387-94.

Adams, F. and A. Rawajfih. 1977. Basaluminite and alunite: a possible cause of sulfate retention by acid soils. *Soil Sci. Soc. Amer. J.* **41**:686-92.

Allison, J.D., D.S. Brown, and K.J. Novo-Gradac. 1991. *MINTEQA2/ PRODEFA2, a geochemical assessment model for environmental systems: Version 3.0 user's manual*. U.S. Environ. Protection Agency, EPA/600/3-91/021.

Balistrieri, L.S., R.F. Ortiz, P.H. Briggs, K.A. Elrick, and P.F. Edelmann. 1996. *Metal fluxes across the sediment-water interface in Terrace Reservoir, Colorado*. U.S. Geol. Survey Open-File Report 96-040.

Ball, J.W., R.L. Runkel, and D.K. Nordstrom. 2001. Reactive transport modeling at high-flow – Wightman Fork/Alamosa River, USA, in R. Cidu (ed.) *Proc. 10th International Symposium on Water-Rock Interaction*, Lisse, The Netherlands, Swets and Zeitlinger 2:1181-84.

Ball, J.W., D.K. Nordstrom, and R.L. Runkel. 2000a. Reactive and Non-Reactive Transport Modeling for Wightman Fork, Summitville Mine, Colorado: Application of the OTIS/OTEQ Model to a Low-Flow Synoptic Study, in Society for Mining, Metallurgy, and Exploration, Inc. (ed.) *Proc. 5th International Conf. on Acid Rock Drainage* 1:125-34.

Ball, J.W., R.L. Runkel, and D.K. Nordstrom. 2000b. A high-flow reactive-transport model of acid mine drainage from Summitville, Colorado based on a June, 1999 tracer injection experiment: *Geol. Soc. Amer. Annual Mtg.*, Reno, NV, Geol. Soc. Amer., A-192.

Ball, J.W., R.L. Runkel, and D.K. Nordstrom. 1999. Transport modeling of reactive and non-reactive constituents from Summitville, Colorado: preliminary results from the application of the OTIS/OTEQ model to the Wightman Fork/Alamosa River system, in D.W. Morganwalp and H.T. Buxton (eds.), *U.S. Geological Survey Toxic Substances Hydrology Program—Proc. Technical Meeting, Charleston, South Carolina, March 8-12, 1999* 1:305-12. U.S. Geol. Survey Water-Resources Invest. Report 99-4018A.

Ball, J.W. and D.K. Nordstrom. 1991. *User's manual for WATEQ4F, with revised thermodynamic data base and test cases for calculating speciation of major, trace, and redox elements in natural waters*. U.S. Geol. Survey Open-File Report 91-183.

Bencala, K.E. and R.A. Walters. 1983. Simulation of solute transport in a mountain pool-and-riffle stream: A transient storage model. *Water Resources Research* **19**:718-24.

Broshears, R.E., R.L. Runkel, B.A. Kimball, D.M. McKnight, and K.E. Bencala. 1996. Reactive solute transport in an acidic stream: Experimental pH increase and simulation of controls on pH, aluminum and iron. *Environ. Sci. Technol.*, **30**:3016-24.

Buchanan, T.J. and W.P. Somers. 1969. Discharge measurements at gaging stations: U.S. Geological Survey Techniques of Water Resources Investigations, book 3, chap. A8.

Camp Dresser and McKee Federal Programs Corporation. 2000. *Response Action Contract for Remedial, Enforcement Oversight, and Non-Time Critical Removal Activities at Sites of Release or Threatened Release of Hazardous Substances in EPA Region VIII. Tier 2 Ecological Risk Assessment Addendum for Summitville Mine Superfund Site, Rio Grande, Conejos, Alamosa Counties, Colorado*. Document Control No. 3280-004-RT-RISK-08992, Golden, Colorado.

Colorado Department of Public Health and Environment. 1998. *Classifications and Numeric Standards for Rio Grande Basin*. Colorado Department of Public Health and Environment, Water Quality Control Commission, Regulation No. 36.

DiToro, D.M. 1976. Combining chemical equilibrium and phytoplankton models - A general methodology, in *Modeling Biochemical Processes in Aquatic Ecosystems* (R.P. Canale, ed.). Ann Arbor, Michigan, Ann Arbor Science, 224-43.

Dzombak, D.A. and F.M.M. Morel. 1991. *Surface Complexation Modeling: Hydrous Ferric Oxide*. John Wiley and Sons, New York.

Kimball, B.A., R.E. Broshears, K.E. Bencala, and D.M. Mcknight. 1994. Coupling of hydrologic transport and chemical reactions in a stream affected by acid mine drainage. *Environmental Science & Technology* **28**:2065-73.

King, T.V.V. 1995. *Environmental Considerations of Active and Abandoned Mine Lands – Lessons from Summitville, Colorado*. U.S. Geol. Survey Bulletin 2220.

Nordstrom, D.K. 1982. The effect of sulfate on aluminum concentrations in natural waters: some stability relations in the system Al_2O_3-SO_3-H_2O at 298 K. *Geochim. Cosmochim. Acta*, **46**:681-92.

Nordstrom, D.K., C.E. Roberson, J.W. Ball, and B.B. Hanshaw. 1984. The effect of sulfate on aluminum concentrations in natural waters: II. Field occurrences and identification of aluminum hydroxysulfate precipitates. Geol. Soc. Am. Ann. Mtg., Oct. 29-Nov. 1, Reno, NV.

Nordstrom, D.K., L.N. Plummer, D. Langmuir, E. Busenberg, H.M. May, B.F. Jones, and D.L. Parkhurst. 1990. Revised chemical equilibrium data for major water-mineral reactions and their limitations, in Melchior, D.C. and R.L. Bassett (eds.) *Chemical Modeling of Aqueous Systems II*, 398-413.

Nordstrom, D.K., J.W. Ball, and R.L. Runkel. 1999. Application of the OTIS/OTEQ transport model to a low-flow study of reactive and non-reactive constituents in Wightman Fork, Summitville Mine, Colorado. AGU Fall Meeting, San Francisco, CA, Dec. 13-17.

Ortiz, R.F. 2001. *Determination of instream metal loads using tracer-injection and synoptic-sampling techniques, Wightman Fork, southwestern Colorado, July 1999*. U.S. Geol. Survey Water-Resources Invest. Report 01-4167.

Ortiz, R.F. and J.W. Ball. 2003a. *Summary of synoptic sampling and tracer-injection tests in the Alamosa River Basin during low-flow conditions, October 1998: A sampling analysis report for modeling reactive transport of metals for the Summitville Mine, Colorado*. U.S. Geol. Survey Open-File Report 03-467.

Ortiz, R.F. and J.W. Ball. 2003b. *Summary of synoptic sampling and tracer-injection tests in the Alamosa River Basin during high-flow conditions, June 1999: A sampling analysis report for modeling reactive transport of metals for the Summitville Mine, Colorado*. U.S. Geol. Survey Open-File Report 03-466.

Ortiz, R.F. and K.E. Bencala. 2000. *Determination of instream metal loads using tracer-injection and synoptic-sampling techniques in Wightman Fork, southwestern Colorado, September 1997*. U.S. Geol. Survey Water-Resources Invest. Report 00-4154.

Ortiz, R.F. and S.A. Ferguson. 2000. *Characterization of water quality in selected tributaries of the Alamosa River, southwestern Colorado, including comparisons to instream water-quality standards and toxicological reference values, 1995-97*. U.S. Geol. Survey Water-Resources Invest. Report 00-4170.

Ortiz, R.F. and R.W. Stogner. 2000. *Diurnal variations in metal concentrations in the Alamosa River and Wightman Fork, southwestern Colorado, 1995-97*. U.S. Geol. Survey Water-Resources Invest. Report 00-4160.

Rubin, J. 1983. Transport of reacting solutes in porous media: Relation between mathematical nature of problem formulation and chemical nature of reactions. *Water Resources Research* **19**:1231-52.

Runkel, R.L. 1998. *One-dimensional transport with inflow and storage (OTIS): A solute transport model for streams and rivers*. http://co.water.usgs.gov/otis/; U.S. Geol. Survey Water-Resources Invest. Report 98-4018.

Runkel, R.L., K.E. Bencala, R.E. Broshears, and S.C. Chapra. 1996a. Reactive solute transport in streams: 1. Development of an equilibrium-based model. *Water Resources Research* **32**:409-18.

Runkel, R.L., D.M. McKnight, K.E. Bencala, and S.C. Chapra. 1996b. Reactive solute transport in streams: 2. Simulation of a pH-modification experiment. *Water Resources Research* **32**:419-30.

Runkel, R.L., B.A. Kimball, D.M. McKnight, and K.E. Bencala 1999. Reactive solute transport in streams: A surface complexation approach for trace metal sorption. *Water Resources Research* **35**:3829-40.

Runkel, R.L. and B.A. Kimball. 2002. Evaluating remedial alternatives for an acid mine drainage stream: Application of a reactive transport model. *Environmental Science & Technology* **36**:1093-1101.

Rupert, M.G. 2001. *Relations among rainstorm runoff, streamflow, pH, and metal concentrations, Summitville Mine area, upper Alamosa River basin, southwest Colorado, 1995-97*. U.S. Geol. Survey Water-Resources Invest. Report 01-4027.

Singh, S.S. 1969. Basic aluminum sulfate formed as a metastable phase and its transformation to gibbsite. *Can. J. Soil Sci*. **49**:383-8.

Singh, S.S. and J.E. Brydon. 1970. Activity of aluminum hydroxy sulfate and the stability of hydroxy aluminum interlayers in montmorillonite. *Can. J. Soil Sci*. **50**:219-25.

Stogner, R.W., P.F. Edelmann, and K. Walton-Day. 1996. *Physical and chemical characteristics of Terrace Reservoir, Conejos County, Colorado, May 1994 through May, 1995*. U.S. Geol. Survey Water-Resources Invest. Report 96-4150.

Stookey, L.L. 1970. Ferrozine - a new spectrophotometric reagent for iron: *Anal. Chem.* **42**:779-81.

To, T.B., D.K. Nordstrom, K.M. Cunningham, J.W. Ball, and R.B. McCleskey. 1998. New method for the direct determination of dissolved Fe(III) concentration in acid mine waters: *Environ. Sci. Technol.* **33**:807-13.

Walton-Day, K., R.F. Ortiz, and P.B. von Guerard. 1995. Sources of water having low pH and elevated metal concentrations in the upper Alamosa River from the headwaters to the outlet of Terrace Reservoir, south-central Colorado, April-September, 1993, in *Proceedings, Summitville Forum '95*, Posey, H.H., J.A. Pendleton, and D.J.A. Van Zyl (eds.), 160-70. Denver, Colorado: Geol. Survey Spec. Pub. 38.

Westall, J.C., J.L. Zachary, and F.M.M. Morel. 1976. MINEQL: A computer program for the calculation of chemical equilibrium composition in aqueous systems. Massachusetts Institute of Technology, Department of Civil Engineering, Tech. Note 18.

Yeh, G.T., and V.S. Tripathi. 1989. A critical evaluation of recent developments in hydrogeochemical transport models of reactive multichemical components. *Water Resources Research* **25**:93-108.